

NSAC/24

January 1981

MASTER

**TMI-2 Accident:
Core Heat-Up Analysis**

DISTRIBUTION OF THIS DOCUMENT IS UNLIMITED

The Nuclear Safety Analysis Center is operated for
the electric utility industry by the Electric Power Research Institute



DISCLAIMER

This report was prepared as an account of work sponsored by an agency of the United States Government. Neither the United States Government nor any agency Thereof, nor any of their employees, makes any warranty, express or implied, or assumes any legal liability or responsibility for the accuracy, completeness, or usefulness of any information, apparatus, product, or process disclosed, or represents that its use would not infringe privately owned rights. Reference herein to any specific commercial product, process, or service by trade name, trademark, manufacturer, or otherwise does not necessarily constitute or imply its endorsement, recommendation, or favoring by the United States Government or any agency thereof. The views and opinions of authors expressed herein do not necessarily state or reflect those of the United States Government or any agency thereof.

DISCLAIMER

Portions of this document may be illegible in electronic image products. Images are produced from the best available original document.

TMI-2 Accident[#]: Core Heat-Up Analysis

NSAC-24

January 1981

Principal Investigators

K. H. Ardron*

D. G. Cain

*On loan to NSAC from CEGB, United Kingdom

Prepared by
Nuclear Safety Analysis Center

Operated by
Electric Power Research Institute
3412 Hillview Avenue
Palo Alto, California 94304

NSAC Project Manager
D. G. Cain

DISTRIBUTION OF THIS DOCUMENT IS UNLIMITED



ORDERING INFORMATION

Copies of this report may be ordered from Research Reports Center (RRC), Box 50490, Palo Alto, CA 94303, (415) 965-4081. There is no charge to NSAC member utilities and certain other nonprofit organizations.

Keywords TMI-2, Core Damage Assessment, Heat-Up Transient

~~Copyright © 1983 by Nuclear Safety Analysis Center~~

NSAC authorizes the reproduction and distribution of all or any portion of this report and the preparation of any derivative work based on this report, in each case on the condition that any such reproduction, distribution, and preparation shall acknowledge this report and NSAC as the source.

NOTICE

This report was prepared by the Nuclear Safety Analysis Center (NSAC) operated by the Electric Power Research Institute, Inc. (EPRI). Neither NSAC, EPRI, members of EPRI, other persons contributing to or assisting in the preparation of the report, nor any person acting on the behalf of any of these parties (a) makes any warranty or representation, express or implied, with respect to the accuracy, completeness, or usefulness of the information contained in this report, or that the use of any information, apparatus, method, or process disclosed in this report may not infringe privately owned rights, or (b) assumes any liabilities with respect to the use of, or for damages resulting from the use of, any information, apparatus, method, or process disclosed in this report.

FOREWORD

PROJECT DESCRIPTION

Much of what happened at TMI-2 is known from parameters that were monitored and recorded. However, there are aspects for which direct indications of plant conditions were fragmentary or unavailable. This is the case for the reactor core conditions, e.g., coolant levels, flows, and fuel temperatures. Although the damage sustained by the core will become known during plant recovery, analysis is required to establish the thermal path by which this condition might have been reached.

This report presents results of an analysis to determine what happened in the reactor core during the critical phase of the accident between 113 and 208 minutes after the reactor tripped. It is during this period that most of the fuel damage is believed to have occurred. Much of the present work is the product of in-house NSAC efforts that are based on a comprehensive study of the TMI-2 accident. Substantial contributions to the analysis were made by contractors assigned to specific problem areas (see references).

PROJECT OBJECTIVES

The objective of this effort was to develop a "best-estimate" thermal-hydraulic analysis of the TMI-2 core heat-up transient. This analysis made use of known boundary conditions, indirect supporting information, and gross indicators of core damage (such as hydrogen production and fission-product release). Many boundary conditions used in the analysis themselves bear uncertainties and require some measure of interpretation. Nevertheless, an effort was made to include all relevant information and subject it to technical evaluations to achieve a consistent whole.

PROJECT RESULTS

A good characterization of TMI-2 core conditions has been achieved for the period from 113 minutes after the reactor trip to 208 minutes. The results are consistent with present estimates of net coolant mass addition to the system, heat

production, and present best interpretations of core instrument responses. Core damage estimates are in reasonable agreement with projections of damage that are based upon hydrogen and fission-product release data. Thus it has been possible to render an accounting of the bulk thermal damage to the core during the TMI-2 accident.

This assessment of core damage does not significantly depart from the range of estimates developed by other, independent studies. However, this work does lend credibility to the position that the core did not experience the high levels of degradation that some have supposed, nor the modest increments of damage which have also been postulated. That appreciable core damage which did occur appears to have been caused by the sustained core uncover and heat-up, such as described by this analysis.

For this analysis it was necessary to build a calculational model from first principles, tailored specifically to the TMI-2 event. Existing general purpose codes suffered from the following limitations: (1) were unable to handle thermal-hydraulic aspects of boil-down which include a closely coupled core-downcomer configuration, (2) were incapable of being generalized to multiregion, core-wide analysis, (3) could not be run efficiently over times that extend over hundreds of minutes for slowly-developing transients, (4) did not feature materials properties, or models of fuel-degradation phenomena, which are important at temperatures in excess of those considered in licensing calculations (1232°C), and (5) tended to use simplifying assumptions which are oriented to worst-case, rather than realistic or best estimate results.

The analysis of TMI-2 core conditions is difficult given the gaps in parts of the data and the limited knowledge of fuel degradation at high temperatures. There are a number of areas which could benefit from further study, and from benchmark observations to be made from the TMI-2 core during plant recovery. This additional information may bear significantly on the present results.

Ongoing work at NSAC and elsewhere is directed at developing the general capability to analyze event sequences which are accompanied by significant core degradation.

D. Cain
K. Ardron
NSAC

ABSTRACT

This report summarizes NSAC study of reactor core thermal conditions during the accident at Three Mile Island, Unit 2. The study focuses primarily on the time period from core uncover (approximately 113 minutes after turbine trip) through the initiation of sustained high pressure injection (after 202 minutes). The transient analysis is based upon established sequences of events; plant data; post-accident measurements; interpretation or indirect use of instrument responses to accident conditions.



CONTENTS

<u>Section</u>	<u>Page</u>
1. Introduction	1-1
2. Modelling of the Liquid Level During Uncovery	2-1
2.1 Model for Predicting Liquid Level in Core	2-1
Calculation of Core Inlet Conditions	2-1
Calculation of Two-Phase Mixture Level	2-4
Numerical Solution	2-6
Experimental Comparison	2-6
2.2 Coolant Addition to TMI-2 Core During Uncovering	2-7
Make-up/Letdown System Operation	2-7
Total Make-up Flow Entering Core	2-14
Operation of the 2B Reactor Coolant Pump at 174 min.	
2.3 Calculated Liquid Level in Core During Uncovering:	
Comparison with Instrument Response	2-16
Time to Fuel Failure	2-19
In-Core Self Powered Neutron Detectors (SPNDs)	2-20
Ex-Core Neutron Detector Response	2-23
3. Modelling of the Thermal Transient	3-1
3.1 Thermal Hydraulic Analysis	3-1
3.2 Zircaloy Oxidation	3-3
3.3 Mechanical Behavior of Fuel	3-4
3.4 Numerical Solution	3-8
4. Calculation of Core Thermal Transient	4-1
4.1 Predicted Fuel Temperatures Over the Period $t = 100-208$ mins.	4-1
4.2 Sensitivity to Input Assumptions	4-6
4.3 Calculated Temperature Transient in the Upper Plenum Region	4-8
4.4 Comparisons with Indicated Level of Core Damage	4-8
Hydrogen Generation	4-10
Fission Product Release	4-12
Instrumentation Behavior	4-18
4.5 Core Behavior After 202 mins: End State Condition	4-19
5. Conclusions	5-1
5.1 Damage Sequence	5-1
5.2 Core End-State	5-2
5.3 Areas of Uncertainty	5-3
Appendix A Calculation of Letdown Flows from Letdown Cooler Outlet Temperatures	A-1
Appendix B Estimates of Steam Condensation Downstream of HPI Nozzles in the TMI-2 Cold Legs	B-1
References	REF-1



LIST OF FIGURES

<u>Figure</u>	<u>Page</u>
1. Schematic diagram of core/downcomer system	2-2
2. Comparison between LEVEL calculations and measured two-phase mixture level in semi-scale test TMI-3I	2-8
3. Schematic diagram of make-up/letdown system showing functional flow paths	2-10
4. TMI-2 primary coolant system	2-11
5. Calculated make-up and letdown flows 100-205 minutes	2-13
6. Assumed distribution of water in reactor vessel immediately after RCP-2B actuation at $\tau = 174$ minutes	2-17
7. Calculated level path during uncovering of TMI-2 core	2-18
8. Location of SPNDs that alarmed high in period $\tau = 166-180$ minutes	2-21
9. Comparison between calculated rate of core heat-up and indications from SPND behavior	2-22
10. Comparison between level trajectories obtained using the thermal-hydraulic and neutron transport calculations	2-24
11. Measured parabolic rate constants for oxidation of zirconium in steam	3-5
12. Results of KFK tests on UO ₂ /Zr-4 pin heat-up to above 2000°C	3-7
13. Longitudinal section of TMI-2 reactor vessel showing axial noding grid used for heat-up analysis	3-9
14. Region boundaries for TMI-2 core heat-up model	3-10
15. Decay heat curve for TMI-2 during period 100-226 minutes from trip	3-16
16. Calculated temperature distribution across core section H and upper phenum at $\tau = 174$ minutes	4-3
17. Calculated temperature distribution across core section H and upper phenum at $\tau = 200$ minutes	4-4
18. Calculated distribution of oxidized Zircaloy in core section H at $\tau = 208$ minutes	4-5

<u>Figure</u>	<u>Page</u>
19. Calculated time variation of mean gas temperature flow rate and steam fraction in the upper plenum at the elevation of the hot leg nozzle	4-9
B1 High pressure injection flow geometry at TMI-2	B-2

LIST OF TABLES

<u>Table</u>	<u>Page</u>
1a. TMI(2) core composition	3-11
1b. Geometric and material parameters used in calculations	3-12
2. Axial and radial variations of fuel rod rating in TMI(2) core	3-13
3. Fraction of fuel mass in different radial regions	3-14
4. Calculated fuel failure time for assemblies in different core regions	4-2
5. Sensitivity of calculated core damage at 202 mins.	4-7
6. Materials inventory in core	4-11
7. Activity releases for TMI(2) fuel	4-13
8. Gap release component	4-15
9. Fission product release by diffusion from UO ₂ matrix	4-16
10. Fission product release from molten UO ₂ /Zr clad in an oxygen deficient atmosphere	4-17



Notation

α_w	Wall area associated with unit subchannel volume
A	Flow area
C_n	Constants in eq (11)
C_ℓ	Specific heat of water
C_p	Specific heat of gas at constant pressure
C_w	Specific heat of fuel element material
d	Subchannel hydraulic diameter
f	Mass fraction of steam in steam/hydrogen mixture
g	Acceleration due to gravity
h	Enthalpy
h_c	Convective heat transfer coefficient
h_{COND}	Condensation heat transfer coefficient at liquid steam surface
j_k	Volumetric flux of phase k
Ku_g	Kutateladze number, defined after (11)
K_p	Rate constant in parabolic rate law
k	Thermal conductivity
M	Mass content
Nu	Nusselt number for subchannel ($=h_c d/k_g$)
p	Width of stream (see Fig. B1)
P	Pressure
Pr_g	Prandtl number ($=\rho_g C_{pg} \nu_g/k_g$)
$q(z)$	Average core rating at elevation z
q_{Ox}	Heating rate/unit subchannel volume due to zirconium oxidation
q_d	Heating rate/unit subchannel volume due to fission product decay
Q_{Ox}	Heat released by oxidation of unit mass of Zircaloy-4
Re	Subchannel Reynolds number ($=U_g d/\nu_g$)
R	Pipe radius
r	A_c/A_{dc}
T	Temperature
t	Time
U	Velocity
V	Volume
W	Flow
x	Distance between injection nozzle and downcomer (Fig. B1)
z	Height above base of active core
z_ℓ	Height of mixture level in core
α_k	Volume fraction of phase k

β_C	Cooler conductance
Γ_k	Rate of absorption of phase k per unit mixture volume
ΔT_{SUB}	Subcooling ($T_{SAT} - T_\ell$)
ρ_k	Density of phase k
τ	Time from reactor trip
σ	Liquid surface tension
η	Condensation efficiency
ν	Kinematic viscosity
μ	Mass of wall material associated with unit subchannel volume

Subscripts

BWST	Borated water storage tank
c	Property of reactor core or core fluid
ch	Property of subchannel
dc	Property of downcomer
e	Fluid entering core
EB	Emergency boration
g	Gas phase or gas mixture
g ℓ	Difference between gas and liquid properties
H	Property of hydrogen
HPI	Make-up to HPI nozzles
i	Property of subcooled flow entering HPI nozzles; also cooler inlet flow
lp	Property of liquid in lower plenum
ℓ	Liquid property
LD	Letdown
o	Outlet property
s	Property of steam; also property of liquid on shell side of heat exchanger
SAT	Saturation property
SI	Pump seal injection
SR	Pump seal return
t	Property of turbulence field; also liquid property on tube side of heat exchanger
TOT	Total flow entering downcomer



SUMMARY

This report describes a best-estimate analysis of the initial core boil-down and heatup transient at Three Mile Island (2) on 28 March 1979. This transient began shortly after all reactor coolant pumps were secured (100 min. after reactor trip) and was terminated by a period of sustained high pressure injection of emergency cooling water, starting at 202 minutes.

The analysis is primarily directed to understanding the progression of core damage, rather than providing a detailed characterization of the core end-state condition. The latter objective can be achieved only after vessel head removal and visual examination.

The thrust of the present effort has been to: (1) develop a core coolant mixture level (dry-out level) calculation which satisfies the boundary conditions implied by various instrument responses and system operational characteristics; (2) couple the level calculation with a core heat-up model to simulate the accumulation of thermal damage in the exposed, upper regions of the core; (3) compare calculated gross damage to the core with measurements of hydrogen and fission product releases subsequent to the accident.

This report provides the principal results from each area of investigation, backed up by sensitivity studies of key parameter variations.

GENERAL CONCLUSIONS

The analysis has shown that the bulk of the core damage at Three Mile Island (2) can be accounted for during the period between 113 min. and 202 min. after reactor trip.

Results indicate that:

- (i) Observed containment hydrogen levels were due to Zircaloy/stainless steel corrosion that occurred during the period of core uncovering between the de-activation of the loop A reactor coolant pump (100 mins after trip) and sustained operation of the high pressure

injection system 100 mins later. Appreciable zircaloy oxidation probably commenced at 150 mins after trip, and continued at a high rate until the sustained high pressure injection at 202 mins caused a major core quench.

- (ii) There was some potential for fuel liquification. Calculations imply that peak fuel temperatures did not exceed the UO_2 pellet melting temperature, but 30% of the fuel was exposed to temperatures where liquid U-Zr-O alloys could have formed.
- (iii) A substantial fission product release was obtained from fuel overheating; however, an apparent disparity between the expected fission product release by calculation and the high range of fission product estimates obtained from plant measurements suggests that a significant release fraction may have originated from powdered or rubbilized fuel during cooldown. Additional gas releases may have developed from hot spots which persisted after core quench.
- (iv) Steam temperatures in the upper plenum, at the outlet nozzle elevation, were generally below $900^{\circ}C$ ($1650^{\circ}F$) although this value was probably exceeded for a few minutes during the partial fuel quench caused by activation of the loop 2B reactor coolant pump, at 174 min after trip. The metal-work in the upper plenum, above the upper tie-plate did not experience appreciable heating.

Thermal damage to the fuel and consequential weakening and mechanical disruption of the core was essentially complete 230 mins after turbine trip.

Section 1

INTRODUCTION

Core damage at the TMI-2 reactor occurred when the core became uncovered because make-up flow was insufficient to compensate for mass loss due to boiling. A prolonged period of uncovering is believed to have taken place during the first 3 1/2 hrs. of the accident [1,2,3]. Because of the subsequent response of radiation monitors inside the reactor containment building it is generally thought that the major part of fuel damage occurred during this period.

Several studies have already been carried out to predict likely peak fuel temperatures and fuel damage in the early period of core uncovering [2,3,4]. However none of the work done so far has attempted to allow for the sequence of actual plant operations that took place over this time. Because of this, no well founded estimates are presently available of the probable extent, and time sequence, of damage sustained by the core and vessel internals during the course of the accident.

The present report is aimed at providing a best estimate of the thermal transient experienced by the reactor core and vessel internals in the early period of uncovering and a general assessment of damage. Such an analysis is desirable at this time to assist recovery and recomissioning efforts at the damaged plant. In addition a calculation of this type provides a useful test of the ability of available analytic methods to describe a reactor accident in which severe core damage occurred.

The work was carried out as part of a NSAC assessment of plant and instrumentation behavior during the accident at TMI-2.



Section 2

MODELLING OF THE LIQUID LEVEL DURING UNCOVERING

The time variation of the boiling mixture level (dry out level) in the core was found to be the most important boundary condition for the core heat up analysis. In this section we outline the arguments that we have used to calculate a best estimate of the level trajectory during the uncovering of the core.

The calculation proceeds in two stages. Firstly a simple loop model is developed to relate the core water level to the make-up flow entering the downcomer. This model is then combined with a best-estimate make-up flow history (developed in Section 2.2) to predict the actual level trajectory at TMI-2. The analysis is an extension of the work presented in [5].

2.1 Model for Predicting Liquid Level in Core

2.1.1 Calculation of Core Inlet Conditions

To calculate the core inlet conditions, the reactor pressure vessel is represented as a simple manometric system divided into three control volumes V_c , V_{lp} , V_{dc} (see Fig. 1). V_c and V_{lp} represent the core volume, and the volume of the lower plenum and downcomer below the elevation of the core base-line, respectively. V_{dc} is the downcomer volume above the core base-line elevation. The core radial reflector region was treated as an integral part of the core, with the same coolant mixture level.

The subcooled makeup flow (w_i) will condense some steam on entering the RCS cold legs. It is not known in general how efficient the condensation will be. However, assuming locally saturated steam, a simple energy balance shows that the total flow of water to the downcomer (injected flow plus condensed steam) can be bounded using the expression:

$$w_{TOT} = w_i \{ 1 + n C_{\ell} (T_{SAT} - T_i) / h_{gl} \} \quad (1)$$

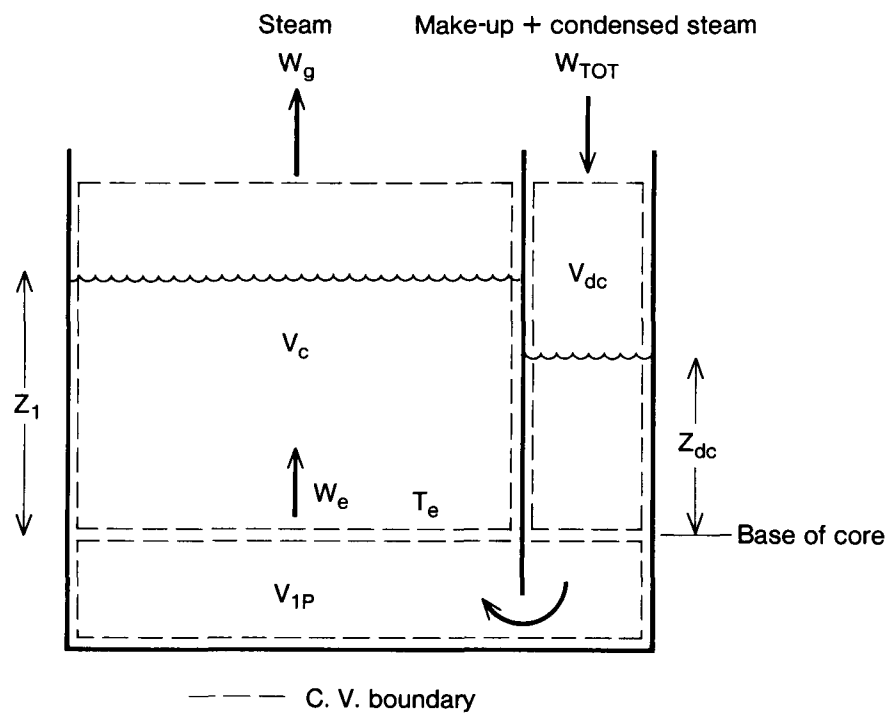


Figure 1. Schematic diagram of core/downcomer system.

Where $0 < \eta < 1$ is the condensation efficiency. For an equilibrium calculation we would take $\eta = 1$. The lower limit $\eta = 0$ describes the limit of complete thermal disequilibrium.

Because of the presence of vent valves between the vessel upper plenum and the downcomer in TMI-2, the steam pressure is assumed to be the same above the fluid columns in V_c and V_{dc} . Balancing the hydrostatic head in these volumes, and neglecting pressure losses due to friction and inertia (which are very small in the slow transient of interest), it follows that:

$$M_c/A_c = M_{dc}/A_{dc} \quad (2)$$

Use of (2) and mass conservation gives the following equation for the liquid flow to the base of the core:

$$W_e = (1 + r)^{-1} (W_{TOT} r + W_g - r\dot{M}_{1p}) \quad (3)$$

The third term on the right hand side of (3) is included to allow for changes in core flow caused by thermal contraction of the lower plenum water. \dot{M}_{1p} is related to the cooling rate by:

$$\dot{M}_{1p} = V_{1p} (\partial \rho_l / \partial T) \dot{T}_e \quad (4)$$

It is assumed that the injection flow mixes instantly with the water already resident in the downcomer/lower plenum volume.* Application of a thermal energy balance to the water in the downcomer and lower plenum then shows that for the limits $\eta = 0$ or $\eta = 1$ the temperature of water entering the core satisfies the differential equation:

*Nominally, some tendency towards thermal stratification can be expected in the lower plenum region; saturated conditions in the lower plenum during the initial boildown period (through 140 min.) and mixing produced when the 2B coolant pump was activated (174 min.) minimizes the importance of this effect.

$$\dot{T}_e = W_{TOT}/M_t [T_i + n (T_{SAT} - T_i) - T_e] \quad (5)$$

The mass of water in the downcomer and lower plenum $M_t (=M_{1p} + M_{dc})$ is given by:

$$\dot{M}_t = W_{TOT} - W_e = (1 + r)^{-1} (W_{TOT} - W_g + r\dot{M}_{1p}) \quad (6)$$

which is obtained by eliminating W_e using (3).

Coolant flashing in the lower plenum during depressurization was considered as part of a scoping analysis, but rejected in comparison to uncertainties attributed to other effects (e.g., condensation/recirculation). Boil-off due to downward radiative heat transfer and axial heat conduction, were excluded on a similar basis.

2.1.2 Calculation of Two-Phase Mixture Level

The mixture height can be calculated if the mass and density of fluid below the mixture level in the core are known.

It follows from (2) and (3) that the mass of fluid in the core below the mixture level satisfies:

$$\dot{M}_c = W_e - W_g = r(1 + r)^{-1} (W_{TOT} - W_g - \dot{M}_{1p}) \quad (7)$$

Assuming all decay heat released below the two-phase level enters the coolant, the core steam production rate can be obtained from a simple energy balance as:

$$W_g = \int_0^{z_\ell} q(z) dz / h_{g\ell} - W_e C_\ell (T_{SAT} - T_e) / h_{g\ell} \quad (8)$$

The second term on the right hand side of (8) represents the energy needed to heat the inlet flow to saturation temperature. Eliminating W_e between (8) and (3) gives the following explicit equation for W_g :

$$W_g = \{i(z_\ell) - \beta r(1+r)^{-1}(W_{TOT} - \dot{M}_{1p})\} / \{1 + \beta(1+r)^{-1}\} \quad (8a)$$

where $i(z_\ell) = \int_0^{z_\ell} q(z) dz / h_{g\ell}$; $\beta = C_\ell (T_{SAT} - T_e) / h_{g\ell}$

To calculate the core mixture level, we first note that

$$M_c = A_c \int_0^{z_\ell} \rho_c(z) dz$$

where ρ_c is the fluid density at elevation z above the base of the core. Differentiating with respect to time, we have

$$\dot{M}_c / A_c = \dot{z}_\ell \rho_c(z_\ell) + \int_0^{z_\ell} \dot{\rho}_c dz \quad (9)$$

For the slow transients of present interest, the second term on the right hand side of (9) is found to be very small compared with the first term and is thus neglected. The mixture height z_ℓ then satisfies the first-order differential equation.

$$\dot{z}_\ell = \dot{M}_c / \{\rho_c(z_\ell) A_c\} \quad (10)$$

Several drift flux models are available to relate the two-phase mixture density $\rho_c(z_\ell)$ to the steam flow-rate at the mixture level (see for example the review in [6]). For the present calculations, we used the correlation proposed by

Cunningham and Yeh [7], which was obtained by analyzing void fraction data from a bundle of 480 PWR rods over a wide pressure range. The correlation has the form

$$\alpha_g = C_1 (\rho_g/\rho_\ell)^{C_2} Ku_g^{C_3} (j_g/j_g + j_\ell)^{0.6} \quad (11)$$

where $C_1 = 0.70$ (0.76), $C_2 = 0.24$ (0.24), $C_3 = 0.67$ (0.47)

for $Ku_g < 1.53$ (≥ 1.53). Ku_g is the non-dimensional steam velocity defined by $Ku_g = j_g / \{\sigma g \rho_\ell / \rho_\ell^2\}^{0.25}$.

In the present case, the steam volumetric flux at the mixture level elevation is related to the core steam production rate by

$$j_g = W_g / \rho_g A_c \quad (12)$$

The mixture density is related to voidage as usual by

$$\rho_c = \alpha_g \rho_g + (1-\alpha_g) \rho_\ell \quad (13)$$

2.1.3 Numerical Solution

The system of three coupled first order ordinary differential equations (5), (6), and (10) are integrated numerically by a simple explicit finite difference procedure in a FORTRAN program, LEVEL. Values of \dot{M}_c and $\rho_c(z_\ell)$ at the current time-step are obtained from conditions at the previous time-step using equations (7), (1), (8a), (4), and (13), (11), and (12) respectively. The power integral $i(z_\ell)$ is obtained by numerically integrating the given power distribution using the trapezoidal rule. Thermodynamic properties of water and steam for the LEVEL calculation are obtained by interpolation from Keenan Keyes steam tables.

2.1.4 Experimental Comparison

There is little data available at present against which to test the two-phase level calculation procedure outlined above. However, some TMI-2 simulation tests have been carried out at the Semi-scale facility in which the core was allowed to

boil down in the absence of make-up flow [8].* Unfortunately, because of the high surface area/volume ratio in Semi-scale, about 80% of the core input power in these tests is dissipated in wall heat losses (this compares with ~4% for TMI-2 in the same time period). Thus, a large fraction of the steam generated in Semi-scale tests recondenses in the system pipe-work, and runs back into the core vessel and downcomer. In test TMI-3I the core uncovered in the period 6400-6900s. The core power was maintained at 125kW up to 6734s and the pressure during uncovering was steady up to this time. Best estimate wall losses for this period are ~100kW of which 80% is from the vessel upper head and external loop pipework [9]. Thus ~80kW of steam generated in the core presumably recondenses and returns to the core/downcomer system.

Figure 2 shows a comparison between the mixture height calculated using LEVEL, and observations for this test, assuming steam re-condensation flows corresponding to heat losses between 75-85kW. Agreement is reasonable, within the uncertainties involved.

2.2 Coolant Addition to the TMI-2 Core During Uncovering

Uncovering of the TMI-2 core is thought to have commenced at about $\tau = 113$ mins. when reactimeter records showed a sudden increase in steam super-heat in the loop-A hot leg. Calculations of the subsequent heat-up transient (see Sections 3 and 4) indicate that the core temperature excursion lasted until about 203 mins., when sustained operation of the high pressure injection (HPI) system caused a major quench of the hot dry fuel.

During the period $\tau = 110$ -203 mins. approximately $2 \cdot 10^4$ kg (5300 gals) water is thought to have entered the reactor core from the make-up/letdown system. An approximately equal mass of water is believed to have been blown into the downcomer annulus over a 10 sec. period by operation of the reactor coolant pump (RCP-2B) at $\tau = 174$ mins. Both of these factors must be included in an estimate of the time varying core water level during the period of uncovering.

2.2.1 Make-up/Letdown System Operation

The makeup flow to the reactor primary system was not measured directly in the TMI-2 plant. However, sufficient data is available on the operation of the

*The small amount of make-up provided to compensate for pump seal leakage rates was ignored in the theoretical comparisons.

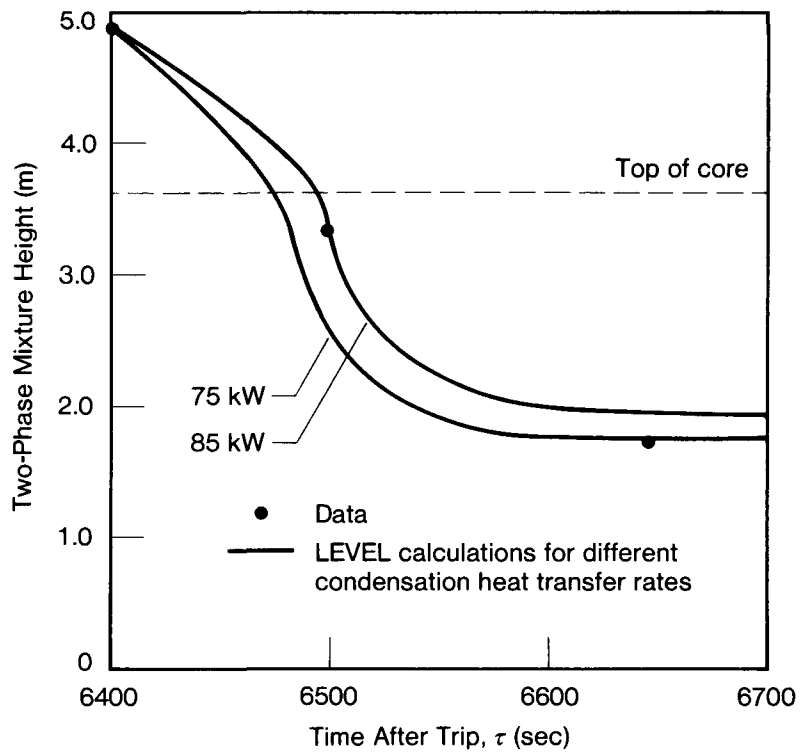


Figure 2. Comparison between LEVEL calculations and measured two-phase mixture level in semi-scale test TMI-3I.

makeup/letdown system during the accident to allow the makeup history to be estimated provided reasonable assumptions are made on valve and pump operation.[5, 10]

Figure 3 shows a schematic diagram of the makeup/letdown system, illustrating the flow paths of interest. (A more detailed account is given in [1].)

Letdown flow is drawn from the base of the reactor A-coolant loop and is directed into either the makeup tank (MUT) or the bleed tank after cooling and throttling to ambient pressure. Additional flow can enter the MUT from the emergency boration tank, pump seal return line, or high pressure pump recirculation line, as shown.

In the manual operating mode, a fixed flow-rate from the outlet of each pump is returned to the MUT via the recirculation line. The remainder is directed back to the RCS as pump seal flow or normal makeup flow. The location of the HPI injection nozzles is shown in Fig. 4.

The flow to the high pressure injection nozzles can be obtained by performing a simple mass balance on the MUT. For conditions where the three way valve, MU-V-8, is positioned to direct letdown flow to the MUT we have (c.f. Fig. 3):

$$W_{HPI} = W_{LD} + W_{SR} + W_{EB} + W_{BWST} - W_{SI} - dM_{MUT}/dt \quad (14)$$

For conditions where MU-V-8 is positioned to divert letdown flow to the reactor coolant bleed hold-up tanks the pertinent equation is:

$$W_{HPI} = W_{SR} + W_{EB} + W_{BWST} - W_{SI} - dM_{MUT}/dt \quad (14-a)$$

Estimates of the contributions on the right hand side of these equations are made below.

(i) Letdown Flows

Although the letdown flow-rate (W_{LD}) was monitored at TMI-2, no continuous record was made for the accident period. However, instantaneous values are available at hourly intervals from the output of the plant log printer [10]. Between these times, variations in letdown flow can be inferred from changes in the temperature of the reactor water downstream of the two

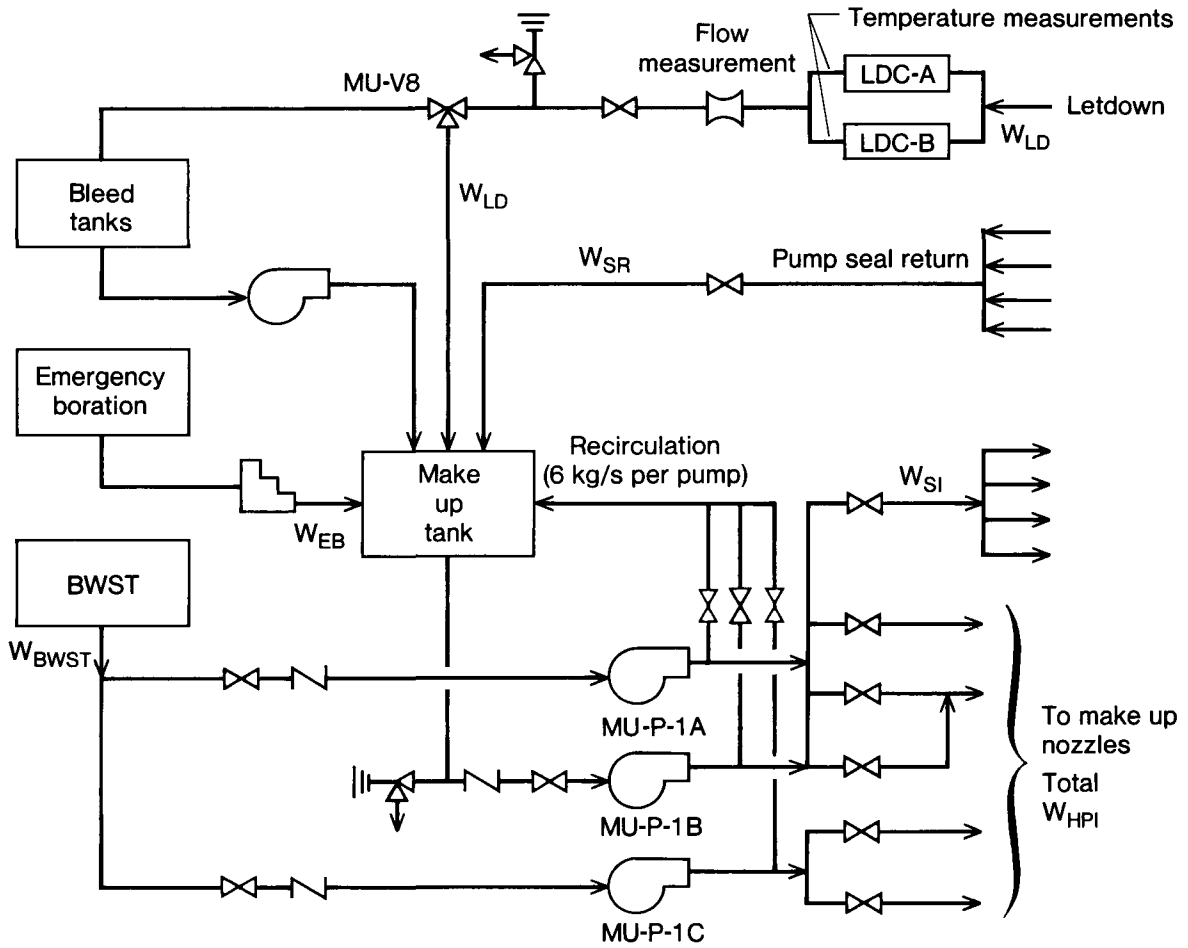


Figure 3. Schematic diagram of make-up/letdown system showing functional flow paths.

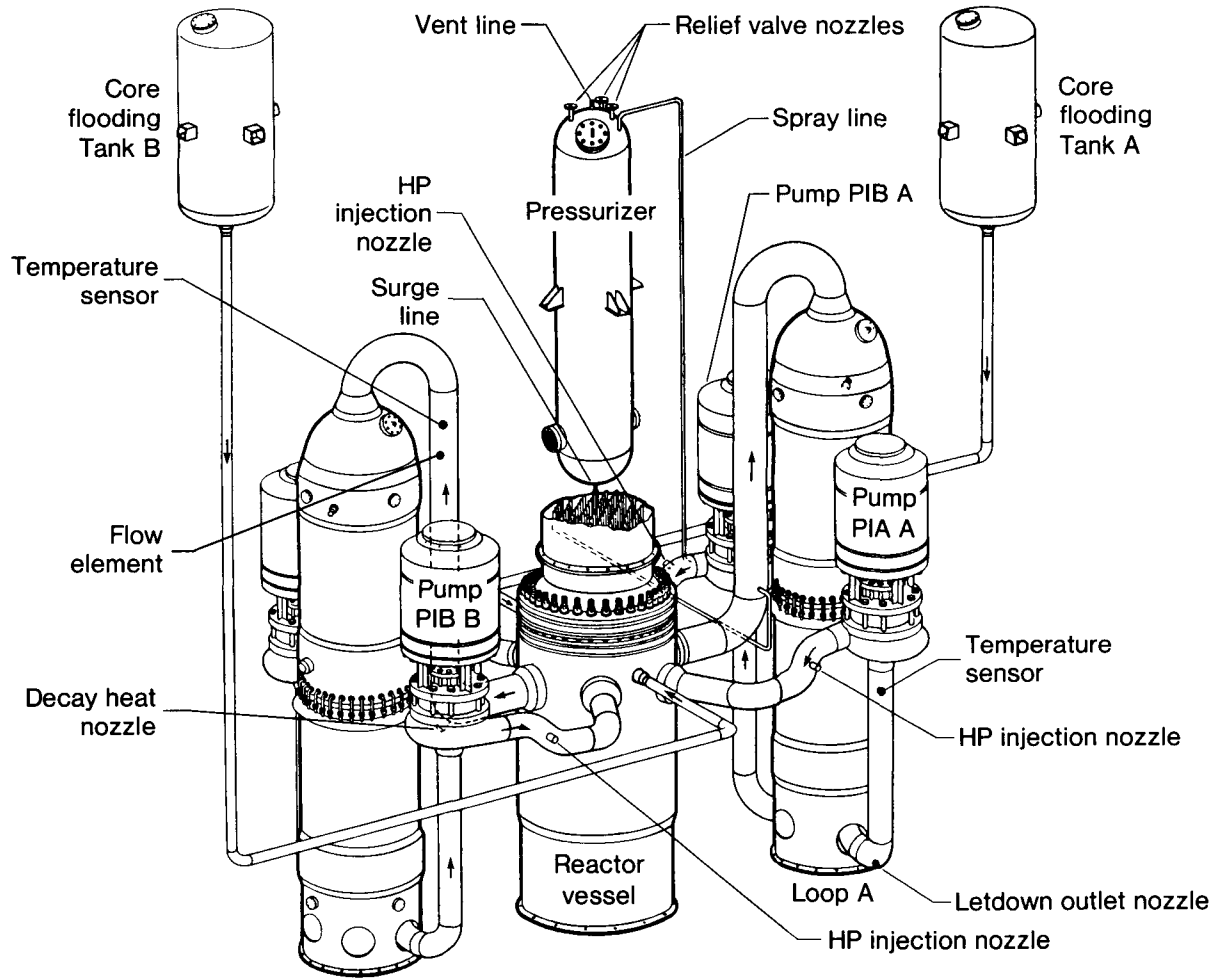


Figure 4. TMI-2 primary coolant system.

letdown coolers, which were recorded continuously on a multipoint recorder [11]. A method of calculating cooler flows from these data is described in [1], and is outlined again in Appendix A. Results of calculations for the period 100-210 mins. are shown in Fig. 5.

(ii) Flow from the Borated Water Storage Tank (BWST)

The BWST (capacity 1790 m³, [4.73·10⁵ gals]) provides the water source for the makeup system in the engineering safeguards (ESF) mode. During the period of the accident between 0< τ <209 mins, 5.5·10⁴kg (14,800 gals) of water is thought to have entered the RCS from the BWST [12]. Output from the alarm printer indicates that the makeup system operated in the ESF mode for a total of 10.2 mins. during this period [10, 12]. Assuming the safety injection system operated at its full design capacity of 63 kg/s (1000gpm), this implies a total injection from the BWST of 3.8·10⁴kg (10,000 gals) during this period of recorded operation. The remaining 1.8·10⁴ kg (4800 gals) was presumably injected in the period 73-166 mins. when the alarm printer was out of action. The manner in which this coolant addition occurred is one of main uncertainties in the present analysis.

A likely mode of operation can be inferred as follows. Operator interviews, and available sequence of events records from the plant computer, indicate that make-up pump MU-P-1C was manually activated soon after $\tau = 101$ mins., and tripped between $\tau = 134-168$ mins. [12,13,14]. This action was taken to provide additional borated water to the reactor to prevent a supposed re-criticality incident [15] (with the known valve line-up MU-P-1C could only draw suction direct from the BWST). Now when a make-up pump is operated manually at low flows a recirculation flow of about 6 kg/s (95gpm) is automatically returned to the MUT [16]. MUT inventory records see Fig. 5 show that changes in dM_{MUT}/dt of almost exactly this magnitude occurred at $\tau = 112$ and 160 mins., which are not obviously traceable to other actions. Assuming these perturbations were caused by activation and trip of MU-P-1C, and assuming a constant suction flow, this implies $W_{BWST} = 6.3$ kg/s (100 gpm) over the period 112< τ <160 mins. This value is adopted for the calculations, and is included in Fig. 5.

(iii) Makeup Tank Inventory

The makeup tank level was recorded at 3 sec intervals during the accident on the reactimeter. The implied rate of change of MUT mass inventory is shown in Fig. 5.

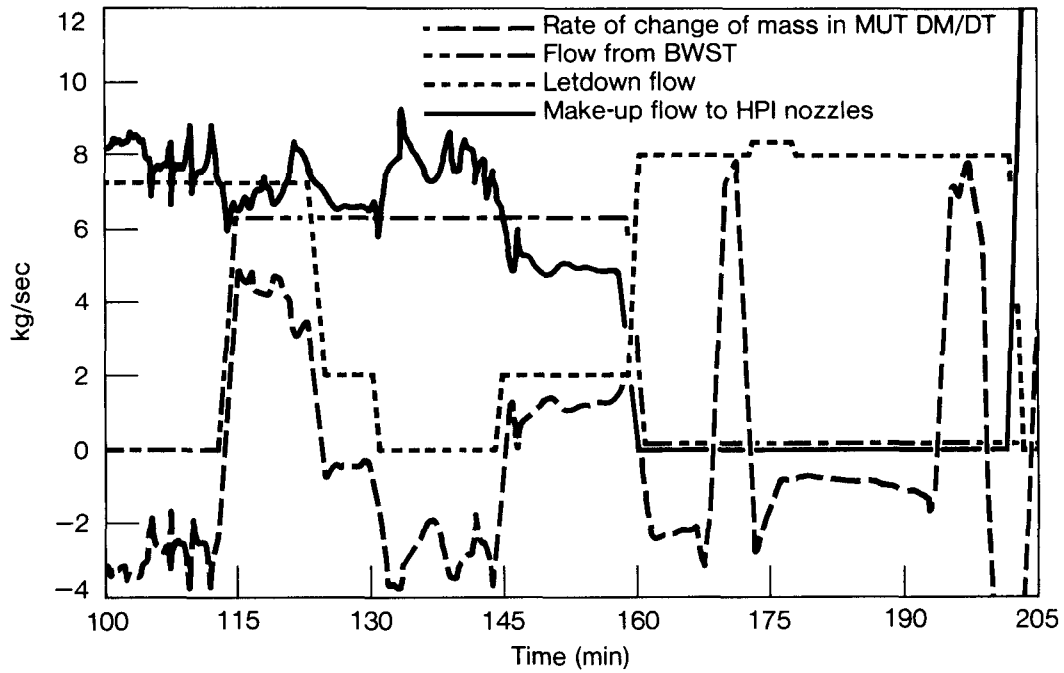


Figure 5. Calculated make-up and letdown flows 100–205 minutes.

(iv) Pump Seal Flow

Pump seal flow is maintained at a constant level $W_{SI}=2.3\pm 0.3$ kg/s (36±4gpm) during plant operation. Seal return flow is $W_{SR}=0.3$ kg/s (4gpm).

(v) Emergency Boration

Flow from the emergency boration tank is 1.3kg/s (20gpm) with two emergency boration pumps in operation. Operator interviews show that emergency boration was carried out intermittently in period $\tau=1-3$ hrs. to prevent a supposed re-criticality incident [10]. Fig. 5 indicates that surges in dM_{MUT}/dt of about 1 kg/s occurred in the periods 134-138 mins. and 141-143 mins. We assume that $W_{EB} = 1.3$ kg/s in these intervals and $W_{EB} = 0$ at other times.

2.2.2 Total Make-up Flow Entering Core

Before the total flow to the HPI nozzles can be estimated judgement must be made on which of Eq. (14) or (14a) is applicable during the period of core uncovering.

Operator testimony [17] suggests that the bleed tanks remained isolated throughout this time and the letdown flow was directed back to the MUT, which indicates that Eq. (14) applies. Up to $\tau = 160$ mins. this is independently confirmed by the observation (see Fig. 5) that each change in letdown flow produces the expected change in the rate of filling of the MUT. However for the period after $\tau = 160$ mins. there is no direct evidence to support the use of either equation. When assessing system behavior to try to establish if Eq. (14a) (letdown diversion) or Eq. (14) (no letdown diversion) were applicable after $\tau = 160$ mins., we found that:

- (i) the high make-up flows implied by (14) are too great to explain the size of fluctuations in injection flow linked to RCS pressure variations after 160 mins. [18].
- (ii) Eq. (14) implies a minimum core liquid level of ~1.5 m, which is 50 cm too high to be reconciled with the observed response of core instrumentation (see 2.3 below).

Also no explanation could be found for the operators to simultaneously increase make-up and letdown at $\tau = 160$ mins., as implied by (14). On the other hand the action to increase letdown and reduce makeup, implied by (14a), is consistent with earlier actions taken by the operators in response to an indication of increasing

pressurizer level*. In view of these arguments we have been led to assume that Eq.(14) applies up to $\tau = 160$ mins. and Eq. (14a) applies thereafter.

The total makeup flow to the HPI nozzles calculated from Eq. (14) and (14a) using the above assumptions for letdown etc., is shown in Fig. 5. The temperature of this feed water is believed to be 32°C (90°F) [17]. Since the HPI nozzles are located below the pump elevation (see Fig. 4), it is assumed that all flow through these nozzles enters the downcomer. However, pump seal flow injection will only spill into the downcomer annulus if the liquid level in the steam generator loops is at the pump elevation. Now the cold leg thermocouples, located upstream of the RCS pumps (see Fig. 4), show a steady temperature decay and indicate substantial temperature noise in both the A- and B-loops in the period $\tau > 120$ mins. [1]. An obvious explanation for this behavior is that thermocouples are positioned in a steam environment, while being bathed continuously in a stream of subcooled water from the pump seals. Because of this, it is assumed that no pump seal flow enters the reactor vessel over the period of interest.

2.2.3 Operation of the 2B Reactor Coolant Pump at 174 min.

At $\tau = 174$ mins. RCP-2B was activated for a 13 minute period, in an attempt to re-establish forced circulation in the primary circuit. During this time the loop-B flowmeter (located in the hot leg, as shown in Figure 4), indicated that forward flow took place for a maximum of 9 sec., commencing at 174.5 mins. The flowmeter response is believed to have been due to the steam displacement caused by the expulsion of a liquid slug from the base of the B loop. If this is so, reactor records of the flowrate indicate that the maximum total mass of liquid injected into the downcomer was $\sim 2.3 \cdot 10^4$ kg ($5 \cdot 10^4$ lbs.). A similar estimate was made in [3].

The sudden quenching of the hot fuel at $\tau = 174$ mins. had a dramatic effect on primary system parameters. Over a five minute period RCS pressure increased from 8.2 MPa to 14.1 MPa (1200-2050 psi) and the pressurizer liquid inventory increased by about 6.5 m³ (230 ft.³). At the same time the loop A and B cold leg thermocouples showed a sudden temperature undershoot, indicating that some fraction of the injected water had bypassed the core, and either entered the A-loop or returned to the B-loop via the RCP-1B.

*The pressurizer level began to rise at $\tau = 147$ mins. after falling fairly steadily from $\tau = 93$ mins.

In modelling the reflood, the assumption was made that the sudden injection of coolant had the effect of filling the downcomer annulus to the elevation of the cold leg nozzles (see Fig. 6); penetration of water into the core over the 10s. injection period was assumed to be negligible (penetration would be inhibited by the greatly accelerated steam generation due to quenching of the over-heated fuel). These assumptions imply that $\approx 12 \text{ m}^3$ of water was added to the core/downcomer system and $\approx 16 \text{ m}^3$ was returned to the loops. To model the subsequent reflood, it was assumed that the liquid levels in the core and downcomer equilibrated over a 5 min. period, in line with indications of RCS pressure records. At the end of the quench period the new core liquid level was estimated by subtracting a coolant boil-off fraction from the core water inventory. The boil-off fraction was calculated by assuming that all the stored energy removed from the newly wetted fuel was converted to heat of vaporization*. The stored energy was calculated in turn from a core heat-up analysis (see Section 3). Effects of entrainment of injected liquid by the steam flow were neglected.

2.3 Calculated Liquid Level in Core During Uncovering: Comparison With Instrument Response.

The subroutine LEVEL was used to calculate the two-phase mixture level in the TMI-2 core for the period of core uncovering out to $\tau = 208$ mins. The mixture level was assumed to reach the core top at $\tau = 113$ mins. (corresponding to the indication on reactimeter records of a sudden increase in steam super-heat in the loop-A hot legs). The make-up flow to the downcomer was assumed to be equal to the HPI nozzle flow (W_{HPI}) in Fig. 5 (c.f. 2.2.2) and the make-up flow temperature was taken as 32°C . The partial reflood at 174 mins. was represented using the assumptions described in 2.2.3.

Decay power for the analysis was taken from calculations for the TMI-2 core provided by B&W [19]. Core average axial power shape was obtained from measurements taken a few days prior to the accident [20].

Results of the LEVEL calculations are shown in Fig. 7, for extreme assumptions of complete thermal equilibrium (maximum condensation of steam on the subcooled make-up flow) and complete non-equilibrium (zero condensation).

*The mass of water boiled off was calculated as 6400 kg (8.5 m^3). This is consistent with the steam production indicated by RCS pressurization and the observed increase in mass content of the pressurizer.

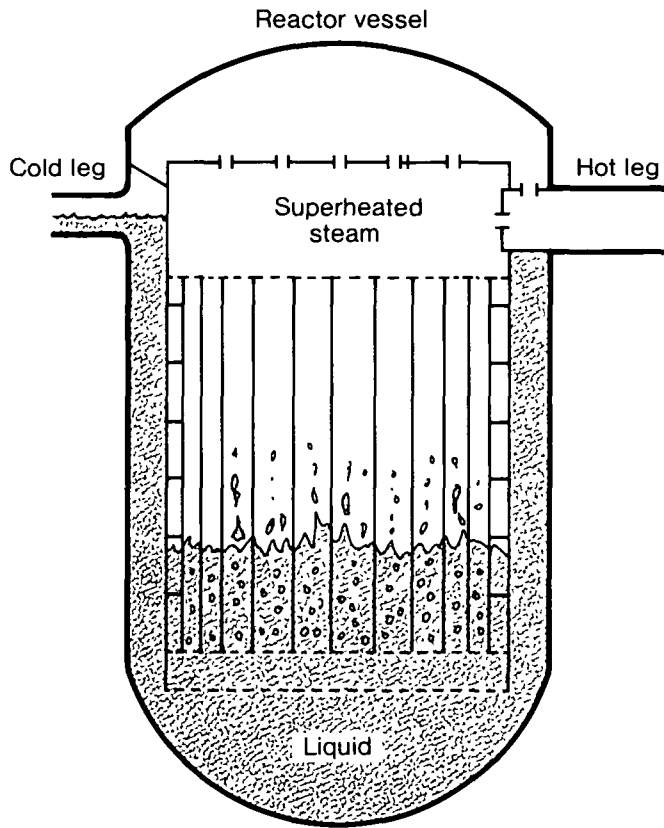


Figure 6. Assumed distribution of water in reactor vessel immediately after RCP-2B actuation at $t = 174$ minutes.

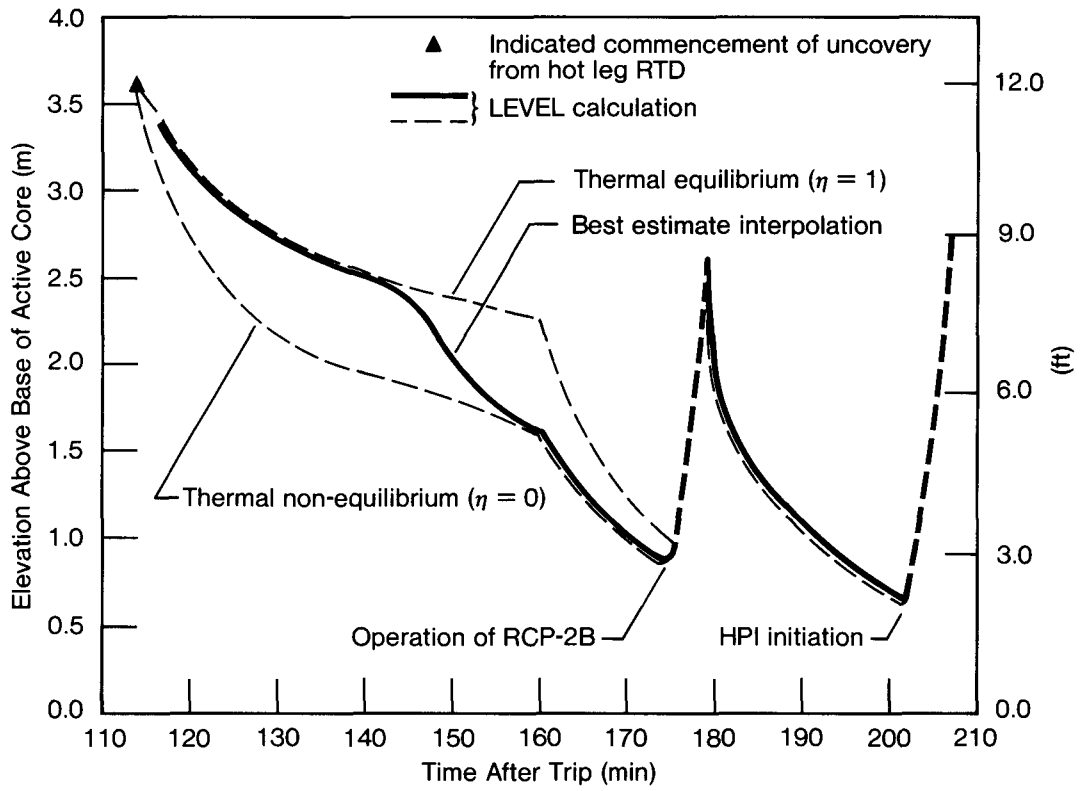


Figure 7. Calculated level path during uncover of TMI-2 core. Solid curve is best estimate calculation.

Appendix B contains some numerical estimates of steam condensation rates on the turbulent liquid stream downstream of the injection nozzles. Results suggest that in the early stages of uncovering the equilibrium ($n = 1$) curve should apply. However, the fuel heat-up calculation detailed in Section 3 indicates that after about $\tau = 142$ mins. significant amounts of permanent gas were released into the core, firstly from fuel pin failure, and subsequently from the zirconium/steam reaction. In the presence of appreciable concentrations of permanent gas, condensation rates would be expected to fall to near zero.* A best estimate curve which allows for this transition is shown as the solid line in Fig. 7.

2.3.1 Time to Fuel Failure

TMI-2 containment monitors showed a sudden increase in radiation levels at $\tau = 145$ mins. [22]. The calculated delay in transport of fission gases from the fuel to the monitors is ~ 3 mins [22], which indicates that progressive fuel cladding failures and fission gas release from plenum and gas regions commenced at about $\tau = 142$ min., (which by coincidence is the approximate time of closure of a block valve downstream of the stuck open electromatic relief valve). The analysis by L. Oakes [22] indicates that fuel failure could not have occurred more than one or two minutes prior to this time, since with the block valve in the open position, containment radiation monitors ought to have been responsive to the failure of just a few tens of fuel pins.

To calculate the fuel failure time implied by the best estimate level transient shown in Fig. 7, this curve was used as an input condition in a full core heat-up analysis. In the calculation, which is described in greater detail in Section 3, the dry fuel is assumed to be cooled by convection to steam released in boiling in the core region below the two phase mixture level. Since steam velocities in the boil down are less than 10 cm sec^{-1} (subchannel Reynolds numbers $< 10^2$) a laminar flow subchannel Nusselt number of four is used to calculate the convective cooling rate.

Fuel failure analyses indicate that the TMI-2 fuel rods would have failed by clad perforation at temperatures between 760°C - 870°C (1250°F - 1700°F) [23,24]. The fuel

*Permanent gas concentrations in excess of a few volume percent can be expected to have an inhibiting effect on the condensation process. Experimental tests [21] have shown a tendency of steam to "sweep" non-condensables to the point of condensation, causing a localized concentration build-up.

heat-up calculation (Section 3) predicts that temperatures in this range (787°C) are first attained at $\tau = 140$ mins. for the peak rated rod, and $\tau = 150$ mins. for the average rod, which agrees with the radiation release observations fairly well.*

2.3.2 In-Core Self Powered Neutron Detectors (SPNDs)

In-core neutron flux levels in the TMI-2 reactor were measured using 364 SPNDs arranged at 7 elevations in 52 instrument strings in the core. The locations of instrumented fuel assemblies in the core are shown in Fig. 14. (Specific details of design and positioning of the instruments are given in [1]). During the period of the accident after $\tau = 110$ mins. the output of many SPNDs became highly anomalous, with output signals going off-scale. It has been found that the off-scale signals are obtained by overheating of instruments and leads above 480°C (900°F) [25, 26].**

The plant alarm printer was out of action for the period $\tau=73-166$ mins. When operation was resumed many alarm signals were received from off-scale SPNDs (i.e., detector currents greater than 2,000 na. or less than -20 na). Results of a statistical analysis of these signals (detailed in [27]) are shown in Fig. 8, for the period $\tau = 166-180$ mins. These data provide convincing evidence that core overheating was confined to elevations above the 0.77 m level, and indicate a probable minimum two phase mixture level of between $z_g = 0.77-1.30$ m. in this time period.

Some SPND signals were displayed on multipoint recorders during the period of uncovering. An analysis of these records can be used to indicate the time variation of the elevation ($z_{480^\circ\text{C}}$) in the core above which the fuel temperature exceeded 480°C, the threshold temperature for the off-scale signals (see ref.

*Sensitivity studies show that because of the effect of compensating reductions in the clad/steam temperature difference at the hot spot, the calculated failure times are changed by less than 0.6% as the Nusselt number is increased from 4 to 20; a representative failure temperature 760°C (1400°F) was used.

**The nature of large positive current signal behavior observed for some SPND's has not been definitively established. A probable explanation has been put forward by Roberts [73], having to do with dielectric thermal relaxation of AlO₂ instrument lead wire insulation above the Curie temperature. The relaxation process releases electrical energy stored in the AlO₂ matrix during normal plant operations, which may result in a positive, if temporary current characteristic during the core heat-up.

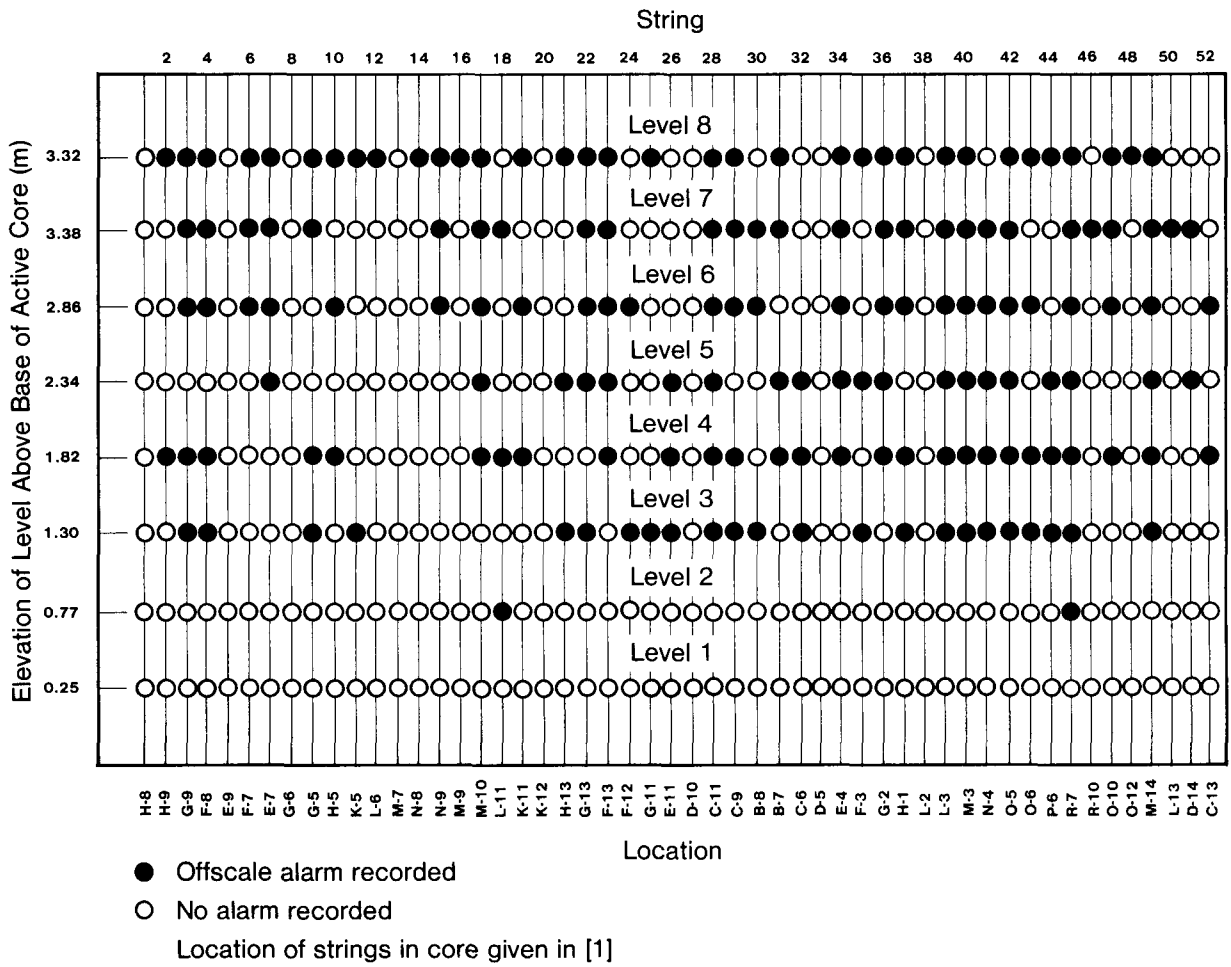


Figure 8. Location of SPNDs that alarmed high in period $\tau = 166-180$ minutes.

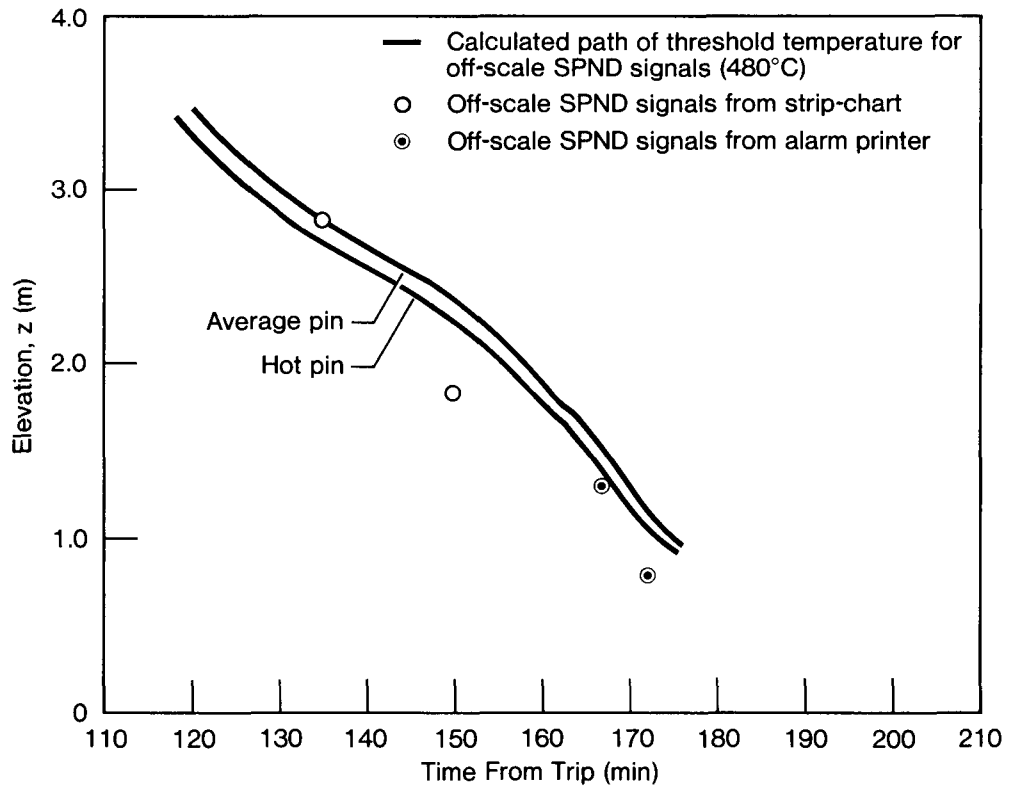


Figure 9. Comparison between calculated rate of core heat-up and indications from SPND behavior.

[27]). The points in Fig. 9 show the indicated path of $z_{480^{\circ}\text{C}}$ based on SPND signals from both the strip-chart and the alarm printer; the curves show the calculated variation of $z_{480^{\circ}\text{C}}$ obtained from the core heat-up analysis, using the level trajectory shown in Fig. 7. Again the calculated level path is seen to be reasonably consistent with the data.

2.3.3 Ex-core Neutron Detector Response

The source range ex-core neutron detector responded to variations in the core water inventory because of competing effects of changes in the core photo-neutron (γ, n) source, and shielding due to the downcomer water [1,29].

A two dimensional (r-Z) neutron transport code DOT-IV has been used to predict the core level implied by the ex-core detector signal. The main assumptions in the analysis (which is detailed in [29]) are that:

- (i) The core is homogenous with a time varying voidage and boron concentration implied by the level history in Fig 7;
- (ii) The normalization constant relating detector response to flux has the unique value required to predict a monotonically decreasing water level.

Results of the calculations are compared with predictions of the thermal hydraulic analysis in Fig. 10. Agreement is very good and is well within the error margin in the transport calculations caused by uncertainties in the detector normalization constant, and the void distribution in the core and downcomer reflector region.

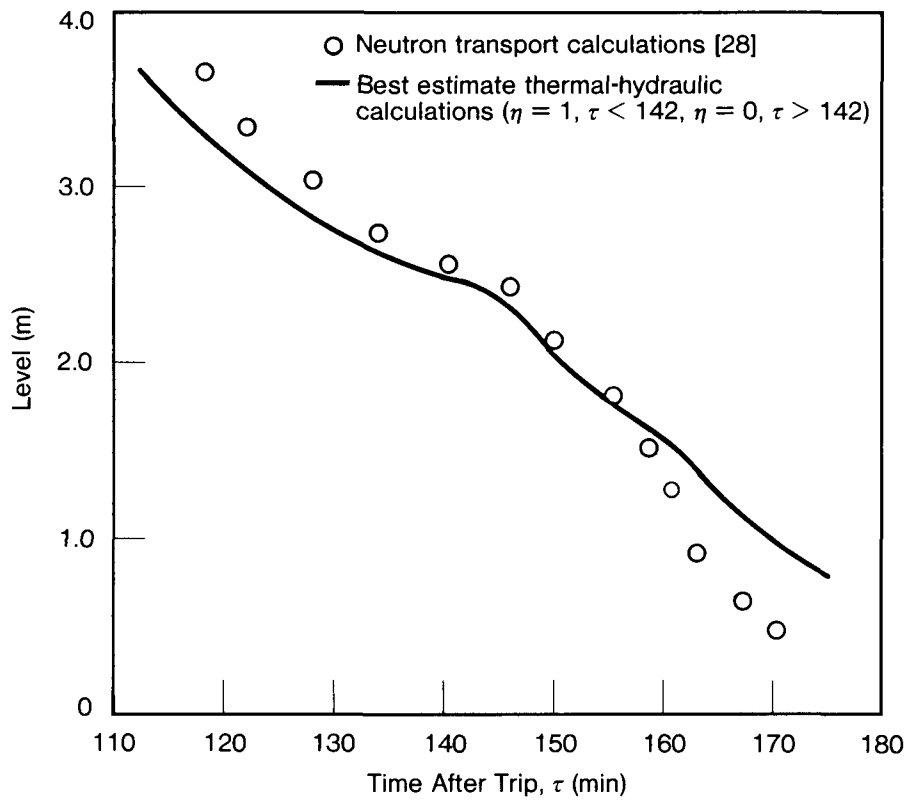


Figure 10. Comparison between level trajectories obtained using the thermal-hydraulic and neutron transport calculations.

Section 3

MODELLING OF THE THERMAL TRANSIENT

The two phase level trajectory calculated in Section 2 was used as a boundary condition in a fuel heat-up analysis. The model used, which is similar to that incorporated into the BOIL code [30] and the TMI Heat-up Code [31], is described below.

3.1 Thermal Hydraulic Analysis

The fuel and metal-structure in the dry region above the mixture level is assumed to be cooled by forced convection to steam/hydrogen mixture derived from bulk boiling in the core below the mixture level. A one-dimensional approximation (no cross-flows) is adopted, so that the flow in each subchannel is assumed to be derived entirely from boiling in the wetted part of the subchannel. In practice, at the low steam velocities characteristic of the boil down (typically 5 cm/s), natural circulation may cause velocity perturbations of magnitude comparable to the bulk flows, in a large open PWR core. The one-dimensional assumption is a simplification adopted in the absence of a detailed description of such three-dimensional flow patterns.

In the dry region, material temperatures are calculated by performing a simple energy balance on the mass of material associated with unit volume of a representative subchannel. This leads to the equation:

$$C_w \frac{\partial T_w}{\partial t} = q_d + q_{ox} - a_w h_c (T_w - T_g) \quad (15)$$

Here q_d , and q_{ox} are the local heating rates per unit subchannel volume that may arise from fission product decay or the zirconium-steam reaction, respectively. The third term on the right hand side is the rate of heat transfer to the steam - hydrogen mixture flowing in the subchannel. (The subscript g here is understood to represent a gas mixture). Eq. 15 neglects property or temperature variations within the fuel, or metal-work (thus no account is taken for example, of possible temperature differences between fuel pellets and cladding in fuel nodes). Axial conduction heat transfer is also neglected since numerical estimates showed that

this is small in the problem of present interest. Heat transfer and bulk fuel heat capacity variations with temperature were included in the analysis.

Radiative heat transfer to steam has been neglected in this analysis since at prevailing low mass flow rates and the enhanced convective heat transfer at high temperatures, steam/gas mixtures readily achieve thermal equilibrium with the fuel. Radiative heat transfer between radial core regions and between the outer-most region and core barrel was not modelled. However, a separate analysis with a modified version of the BOIL code [33] has shown this heat transfer mechanism to have no appreciable effect.

In the wetted region it is assumed that the fuel rods remain at the saturation temperature. The gas temperature in the dry region is obtained by solving one-dimensional equations for mass and energy conservation. (Momentum losses are ignored since flow velocities in boil-down are generally very small). Considering an individual subchannel, the pertinent equations are:

$$\frac{\partial}{\partial z} (\rho_g U_g) + \frac{\partial \rho_g}{\partial t} + \Gamma_g = 0 \quad (16a)$$

$$\rho_g U_g \frac{\partial T_g}{\partial z} + \rho_g \frac{\partial T_g}{\partial t} = a_w h_c (T_w - T_g) \quad (16b)$$

Where Γ_g is the rate of mass absorption per unit volume that arises because of possible chemical reaction between the steam and the Zircaloy-4 cladding of fuel rods. (see Section 3.2 below).

The dominant heat transfer mechanism in the present analysis is assumed to be forced convection. The heat transfer coefficient was taken from standard text book correlations for forced flow in tubes [34]:

$$\begin{array}{ll} \text{Nu} = 4 & \text{Re} < 2000 \\ \text{Nu} = 0.023 \text{Re}^{0.8} \text{Pr}^{0.3} & \text{Re} > 2000 \end{array}$$

Where Re is the subchannel Reynolds number.

The boundary conditions for Eq. 16 are, at $z = z_\ell$, $T_g = T_{sat}$ and

$$U_g = (\rho_g h_{gl})^{-1} \left[\int_0^{z_\ell} q_d(z) dz - W_e \Delta T_{sub,e} / A_c + C_w \dot{z}_\ell (T_w - T_{sat}) \right] \quad (17)$$

The three contributions to steam generation below the mixture level shown in (17) are: (i) the decay power; (ii) the power required to raise the core inlet water to saturation temperature; and (iii) the rate of heat released in quenching the dry fuel. Contribution (iii) is set to zero in boil-down, but can be very large in refill.

Properties of the steam-hydrogen mixture are expressed as mass weighted averages. Thus

$$C_{pg} = f C_{ps} + (1-f) C_{pH} \dots \text{etc.} \quad (18)$$

where f is the local mass fraction of steam. Consideration of mass conservation for the steam component shows that f satisfies the differential equation:

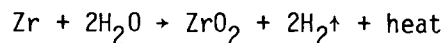
$$\rho_g U_g \frac{\partial f}{\partial z} + \rho_g \frac{\partial f}{\partial t} = (f \Gamma_g - \Gamma_s) \quad (19)$$

which can be integrated along the subchannel.

Property values for the steam and hydrogen components are obtained as a function of P and T_g from tables [35].

3.2 Zircaloy Oxidation

In high temperature steam the Zircaloy-4 fuel rod cladding is oxidized in an exothermic reaction [33].



The heat released is $Q_{ox} = 6.45 \cdot 10^6$ Joule per kilogram of reacted zirconium.

For the present analysis the heat of oxidation in Eq. (15) is calculated from the equation:

$$\begin{aligned} q_{\text{ox}} &= 0_{\text{ox}} \partial\mu/\partial t & f > 0 \\ q_{\text{ox}} &= 0 & f = 0 \end{aligned} \quad (20)$$

Where μ is the zirconium mass per unit subchannel volume. Eq. (20) allows for the fact that oxidation cannot proceed once the steam flow in a subchannel is completely reduced to hydrogen (steam starvation limit).[37]

The rate of reaction is obtained from a standard parabolic rate law:

$$W^2 = K_p t + \text{const.} \quad (21)$$

Here W is the weight of reacted zirconium per unit surface area at time t . The rate constant K_p is obtained from best-estimate empirical correlation of the form [37, 38, 39]

$$K_p = A e^{-B/T} \quad (22)$$

where

$A = 0.932 \text{ (kgZr)}^2\text{m}^{-4}\text{s}^{-1}$	$B = 1.38 \cdot 10^4 \text{ }^\circ\text{K}$	$T < 1090 \text{ }^\circ\text{K}$
$A = 294 \text{ (kgZr)}^2\text{m}^{-4}\text{s}^{-1}$	$B = 2.01 \cdot 10^4 \text{ }^\circ\text{K}$	$1090 < T < 1850 \text{ }^\circ\text{K}$
$A = 114 \text{ (kgZr)}^2\text{m}^{-4}\text{s}^{-1}$	$B = 1.67 \cdot 10^4 \text{ }^\circ\text{K}$	$1850 \text{ }^\circ\text{K} < T$

Fig. 11 shows that these correlations give a reasonable representation of typical data for the oxidation of Zircaloy specimens in steam.

In our analysis only oxidation at the outer pin surfaces is considered. Estimates by Coleman [25] suggest that oxidation of inner cladding surfaces contributes only small fractional increases in heat production and H_2 generation.

3.3 Mechanical Behavior of Fuel

There is very little experimental data on the mechanical performance of fuel assemblies under the extreme thermal transients of present interest. However an analysis has been performed using the FRAP-T5 code to estimate clad ballooning

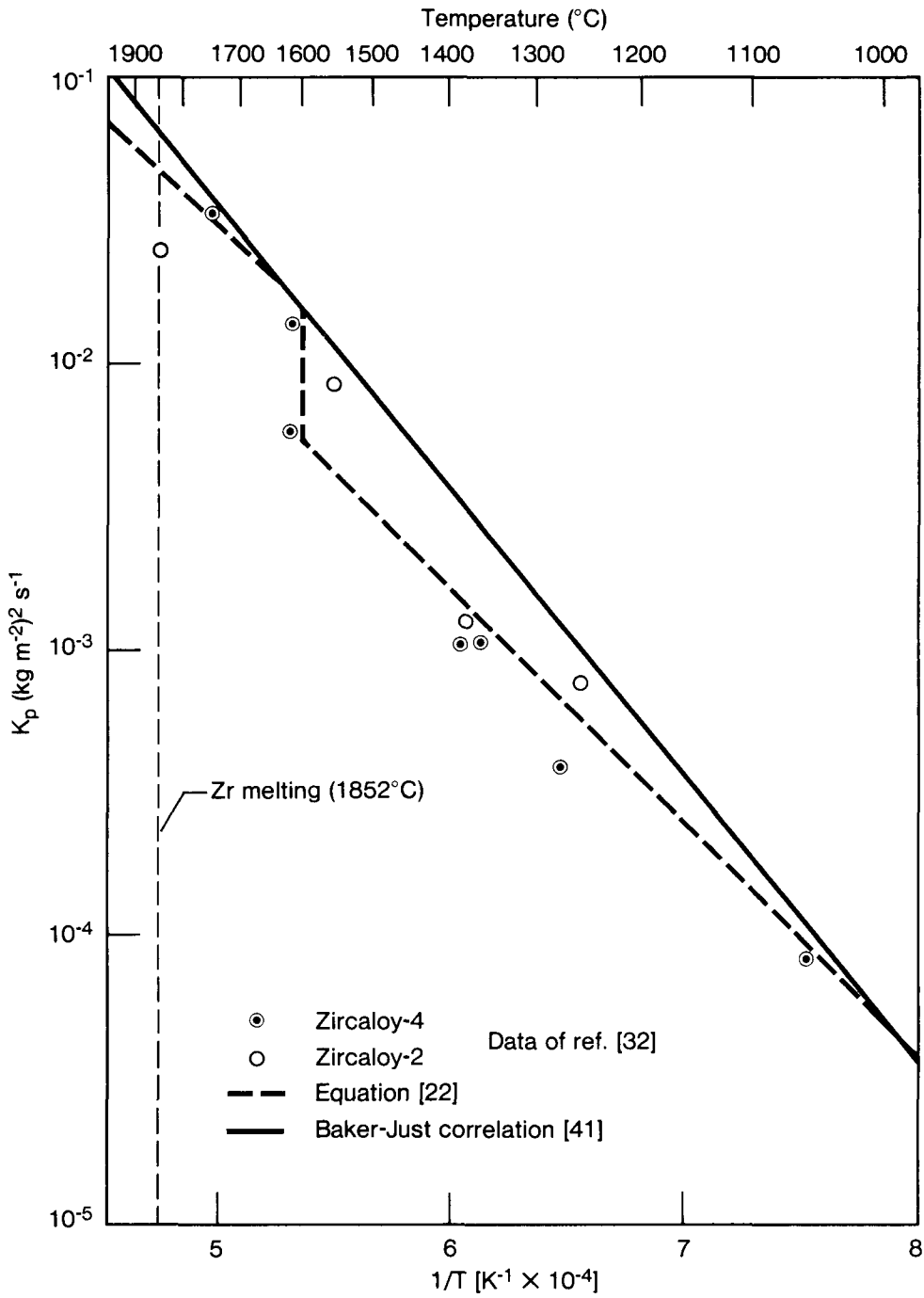


Figure 11. Measured parabolic rate constants for oxidation of zirconium in steam.

behavior for the pressure and fuel temperature transients characteristic of the TMI-2 accident [25]. Results indicate that only limited clad deformation (strains less than 15%) occurs prior to pin rupture, which is estimated to take place at temperatures between 760-870° C (1400-1600°F). The relatively small calculated failure strains are a consequence of the fact that the differential pressure across the clad remains comparatively small while the clad is heated through the ductile α -phase.

As the temperature continues to rise liquification of core materials would be expected to take place. The first material to melt would probably be the Ag-In-Cd alloy control rod material, which has a melting point of 810°C (1800°F). Release and flow of this liquified alloy would be expected to occur at about 1400°C, when oxidation and melting would cause failure of the stainless steel control rod cladding. Henry [42] has suggested that subchannel blockages (and hot-spots) might be caused by the refreezing of the alloy. However, since only 7% of the pins in each fuel assembly are in the form of control rods, the potential for core-wide heat transfer impairments is small.

As temperatures begin to approach the melting point of Zircaloy (1850°C), properties of the fuel rods will start the change. Tests at KFK have been carried out using electrically heated fuel pin simulators to examine clad pin-coolant interactions at temperatures up to and exceeding the clad melting point (1850°C) [41]. Results show that above the clad melt temperature liquified alloy "eutectic" mixtures can form between the zirconium and the UO_2 fuel pellets. At the moderate clad heating rates calculated for the TMI-2 fuel ($\dot{T}_w \sim 0.5 - 2.0^\circ C/sec$) it was found in these tests that during heat-up the outer ZrO_2 layer on the fuel cladding is usually thick enough to be stable against penetration by the liquified eutectic, which remains confined within the fuel pin. (Our calculations indicate that prior to clad melting, typically 30% of the outer clad zirconium is oxidized).* However the tests also indicate widespread disruption of the oxide layers during cool-down. (Typical results are illustrated in Fig. 12).

These considerations indicate that blockage effects due to flow of liquified materials was probably fairly small in the early uncover phase. However, the quenching events at 174 and 202 mins would probably have caused some blockages

*The oxidation fraction considered here is a local property that may have been significantly influenced by the presumption of a steam starvation effect.



Figure 12. Results of KFK tests on $\text{UO}_2/\text{Zr-4}$ pin heat-up to above 2000°C .
(a) $T = 4^\circ\text{C}/\text{sec}$ UO_2/Zr eutectic penetrates clad during heating;
(b) $T = 2^\circ\text{C}/\text{sec}$ clad integrity maintained in heating but fracture occurs in cooling;
(c) $T = 0.25^\circ\text{C}/\text{sec}$ clad integrity maintained in both heating and cooling.

through clad shattering and debris formation. Embrittlement data in (43) suggests that clad shattering due to mechanical or thermal shock is likely when the oxygen uptake of the Zircaloy exceeds 20 percent. Our calculations (4.1 below) indicate that at 174 mins, Zircaloy above this embrittlement limit was confined to the central fuel assemblies above the 3m. elevation (under 10 percent of the core volume) suggesting that debris formation due to the early quench was small. In contrast to this it is estimated that by 200 mins over 70 percent of the cladding had probably exceeded the embrittlement threshold.

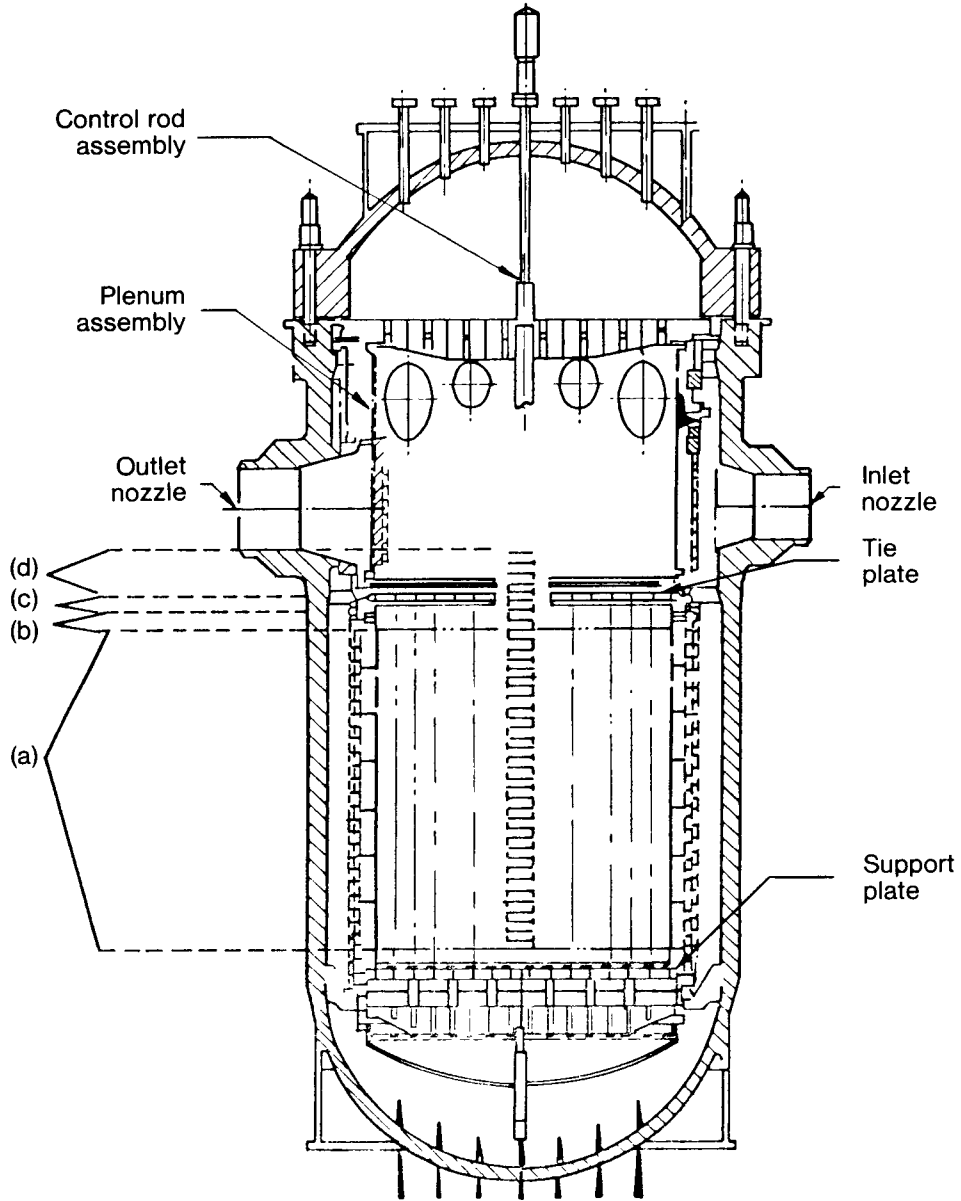
The implication is that flow blockage effects were probably small at TMI-2 up to 200 mins after trip, but that a major rearrangement in core geometry occurred after this time. Accordingly we have ignored heat transfer perturbations due to blockage in calculating the heating transient in the period 113-200 mins.

3.4 Numerical Solution

Equations (15) (16) (19) and (20) were integrated by an implicit finite difference procedure in a FORTRAN program to calculate temperatures during the core uncovering. The level trajectory, and the values of $\Delta T_{SUB,e}$ and W_e needed as a boundary condition for the calculations were obtained from the core liquid level analysis.

For the numerical calculations the region between the base of active core and the elevation of the hot leg nozzles was divided axially into 40 nodes, each 11.4 cm (4.5 in) in length. The noding arrangement is shown in Fig. 13. Material properties in the fuelled and non-fuelled regions of the rod assemblies (nodes 1-32, and 33-36 respectively) were estimated from published data (see ref. [43]). Material properties and geometric data for the upper plenum region are based on unpublished data provided by B&W [41]. Code input data is summarized in Tables 1a and 1b.

The spatial distribution of decay power in the active core was allowed for by dividing the core into eight radial regions, such that the individual bundle power in each region differed from the region average by under 15%. Accurate representation of the decay power distribution in the core has a significant bearing upon the temperature distribution above $\sim 1100^\circ\text{C}$ and the assessment of bulk core damage. The power distribution data were provided by Thomas [45], and are based on measurements made by B&W in the days prior to the TMI-2 accident [20]. Fig. 14 shows the boundaries of the radial zones (each grid square represents an indivi-



Key

- Region (a) nodes 1-32: active core
- Region (b) nodes 33-34: rod plenum region
- Region (c) nodes 34-36: upper tie plate/assembly end fittings
- Region (d) nodes 36-40: upper plenum region

Figure 13. Longitudinal section of TMI-2 reactor vessel showing axial noding grid used for heat-up analysis.

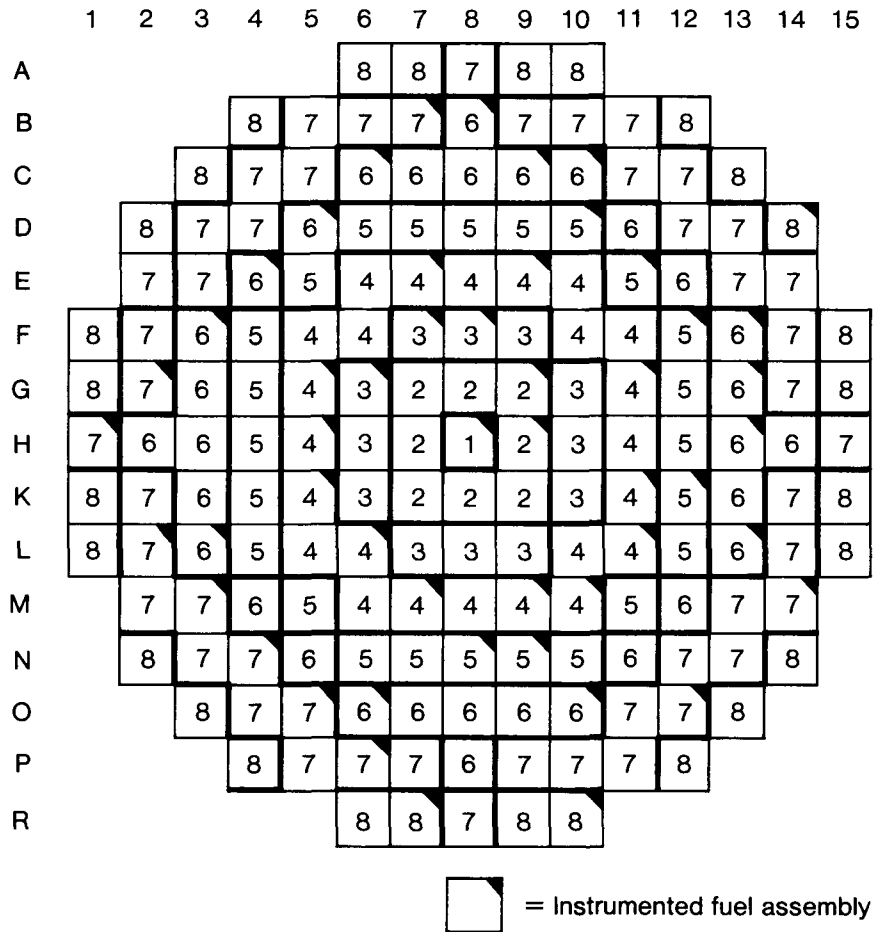


Figure 14. Region boundaries for TMI-2 core heat-up model.

TABLE 1a
TMI(2) core composition

Region Axial Extent (from base of active core) (m)	Assumed type of material occupying region	Mass/unit subchannel volume of materials of different types (4)				Heat (4) transfer area per unit sub- channel volume (m ² /m ³)	Heat capa- city per unit sub- channel volume (J/m ³ °C)	Reference for source data
		UO ₂ (kg m ⁻³)	Zr-4 (kg m ⁻³)	304-SS (kg m ⁻³)	TOTAL (kg m ⁻³)			
0-3.66	Zr-4/UO ₂ Fuel Rods	6122	1240	-	7362	298	(1)	[43]
3.66-3.86	Rod Plenum Region	-	1240	776	2016	298	(1, 2)	[43]
3.86-4.01	Stainless Steel Assembly End-Fittings /Upper Core Tie Plate	-	-	9450	9450	220	(2)	[43]
4.01-4.57	Upper Plenum Region/Control Rod Guide Assemblies	-	-	(3)	(3)	(3)	(2)	[44]

TABLE 1a - Material properties in the different axial regions assumed for calculations.

NOTES:

1. Calculated from temperature dependent properties of Zr-4 and UO₂.
2. Calculated from temperature dependent properties of type 304-SS.
3. Data Proprietary to B&W.
4. Based on subchannel area at $1.15 \times 10^{-4} \text{ m}^2$

TABLE 1b

Core Flow Area (A_c) (Includes reflector region)	5.94 m ²
Downcomer Area (A_{dc})	3.94 m ²
Lower Plenum Volume	25.7 m ³
Subchannel Area	1.15 x 10 ⁻⁴ m ²
Fuel pin o.d.	1.092 cm
Glad Mass/unit pin length	0.142 kg/m
UO ₂ mass/unit pin length	0.704 kg/m

Table 1b Geometric and material parameters used in calculations.

TABLE 2

Radial Region Z (m)	1	2	3	4	5	6	7	8
3.40	5.38	4.78	4.78	4.49	4.10	4.24	3.50	2.18
2.87	9.14	8.35	8.24	8.14	7.78	7.80	6.36	4.24
2.35	10.24	9.20	8.93	8.46	7.67	7.96	6.75	4.69
1.83	10.74	9.24	8.87	7.90	6.59	7.08	6.47	4.56
1.31	11.00	9.16	8.69	7.94	6.70	7.20	6.51	4.56
0.785	10.28	8.54	8.13	7.87	7.26	7.56	6.38	4.36
0.262	6.72	5.66	5.48	5.27	5.09	5.19	4.24	2.81

TABLE 2 - Axial and radial variations of fuel rod rating
in TMI-2 core (in kw/ft) for 98% full power
{2720 MW(th)}

TABLE 3

RADIAL REGION	FRACTION OF TOTAL FUEL MASS IN REGION (%)
1	0.565
2	4.52
3	6.78
4	13.56
5	13.56
6	18.08
7	27.12
8	15.82

TABLE 3 - Fraction of fuel mass in different radial regions.

dual fuel assembly), and Tables 2 and 3 give the power distribution data and fuel mass fractions for each zone.

The absolute core power levels during uncovering were obtained from a decay curve calculated by B&W for the TMI-2 core (see Fig. 15).

Total core damage in the fuelled region was computed by performing heat up calculations for the eight regions individually, and then summing the results to give a weighted mean. Thus, if the calculated fraction of clad oxidized in the i^{th} radial zone is $f_{\text{ox}}^{(i)}$ then the core average would be defined by

$$\bar{f}_{\text{ox}} = \sum_{i=1}^8 f_{\text{ox}}^{(i)} W^i$$

where W^i are the weight fractions given in Table 3.

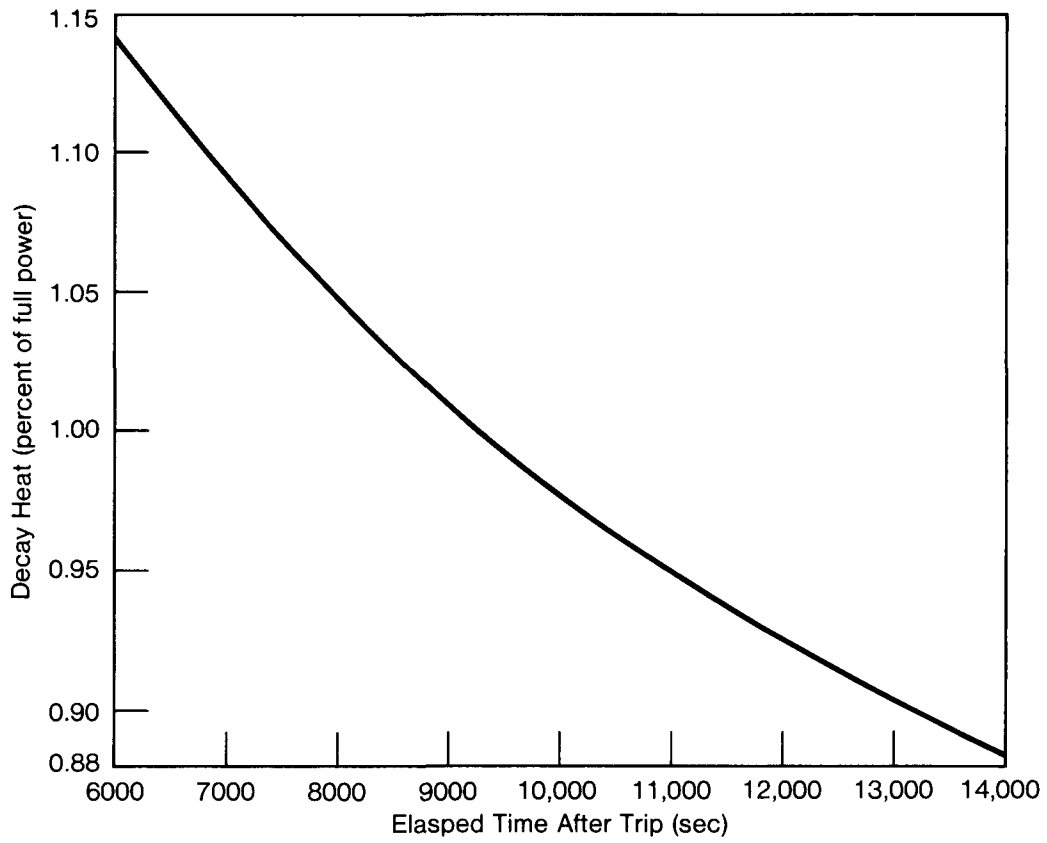


Figure 15. Decay heat curve for TMI-2 during period 100–226 minutes from trip.

Section 4

CALCULATION OF CORE THERMAL TRANSIENT

The model outlined in Section 3 was used to calculate the core temperature distribution and assess fuel behavior for the period of core uncovering. The level trajectory for the base calculations is that shown in Fig. 7. The calculational results and implications with respect to core damage and end-state condition are described in this section.

4.1 Predicted Fuel Temperatures Over the Periods $\tau = 100-208$ mins.

The predicted failure times for the fuel in the different radial zones are listed in Table 4; these figures are based on the assumption failure occurs in the temperature range 760-870°C.

Fig. 16 shows the calculated distribution of isotherms across the central core section H1-H15 (see Fig. 14) and the corresponding section of the upper plenum, prior to activation of RCP-2B at 174 mins. The region where embrittlement has occurred (i.e., the region where zircaloy oxidation exceeds 20%) is also shown in Fig. 16. The total core wide zircaloy oxidation at this time is calculated to be 12%, and the peak fuel temperature in the center assembly is 2650°C (4800°F), which is close to the melting temperature of the fuel. Maximum fuel pin temperatures occurring during the transient are calculated to occur at this time.

Temperature reductions of the dry fuel, due to forced convective cooling by the steam released in the refill at 174 mins, are calculated to be ~850°C. This cooling effect is transitory, and core heatup is resumed when the injected fluid has been substantially boiled off. Fig. 17 shows the new pattern of isotherms at 200 mins, prior to initiation of high pressure injection.

It is calculated that by 208 mins., fuel temperatures are falling rapidly, and the oxidation process is effectively terminated. The total zircaloy oxidation above the active core base at this time is estimated to be 39%; Fig. 18 shows the predicted distribution of oxidized material. The unexpected prediction of layers of different composition is a consequence of the assumption used in the analysis

TABLE 4

CORE RADIAL REGION	CALCULATED FUEL FAILURE TIME (mins)
1	140 - 156
2	147 - 157
3	148 - 158
4	149 - 157
5	150 - 159
6	151 - 159
7	156 - 162
8	162 - 168

TABLE 4 - Calculated fuel failure time for assemblies in different core regions (based on assumption that failure temperature is in range 760 - 870°C)

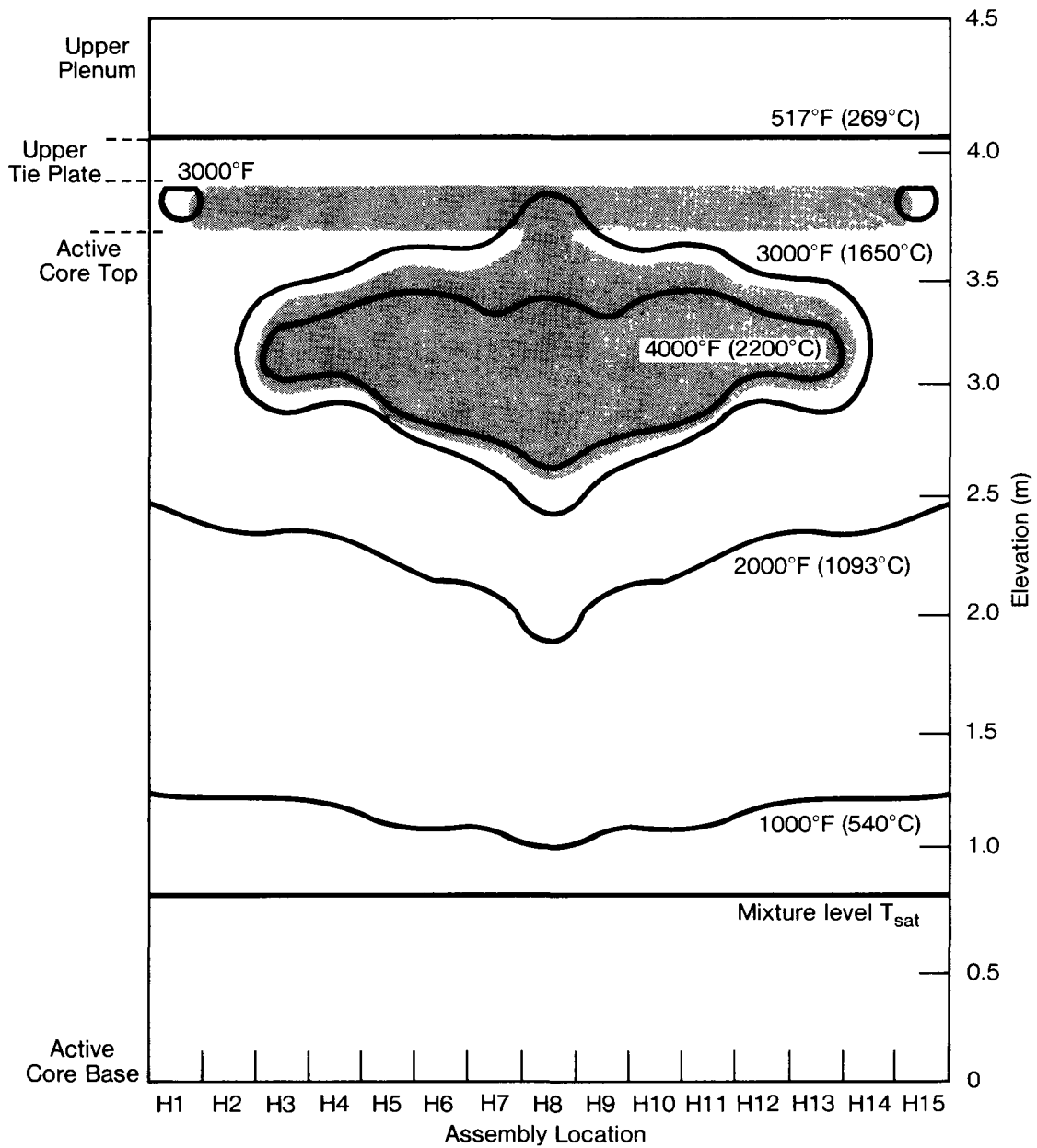


Figure 16. Calculated temperature distribution across core section H and upper plenum at $\tau = 174$ minutes. (Shaded area denotes region of clad embrittlement).

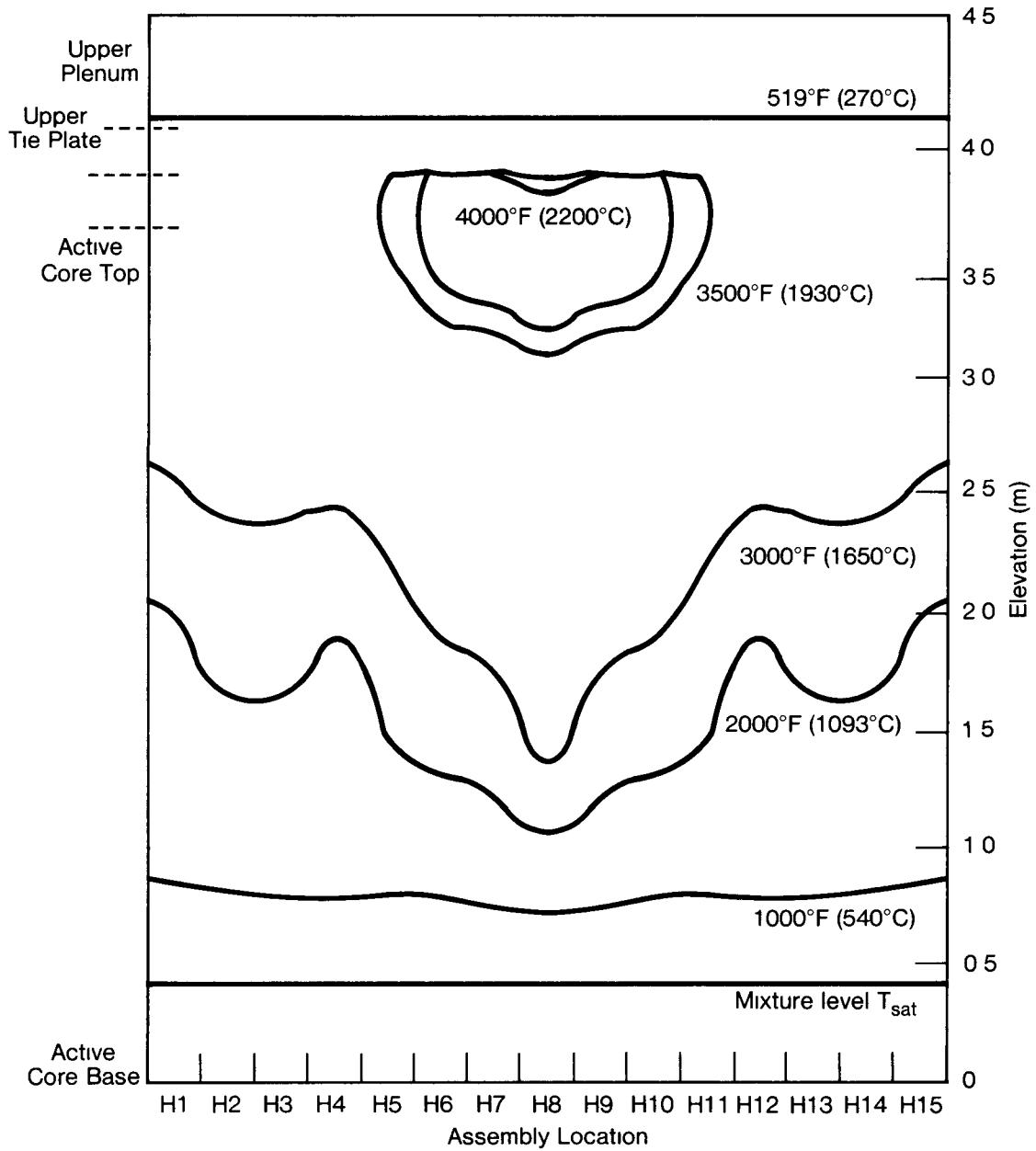


Figure 17 Calculated temperature distribution across core section H and upper plenum at $\tau = 200$ minutes

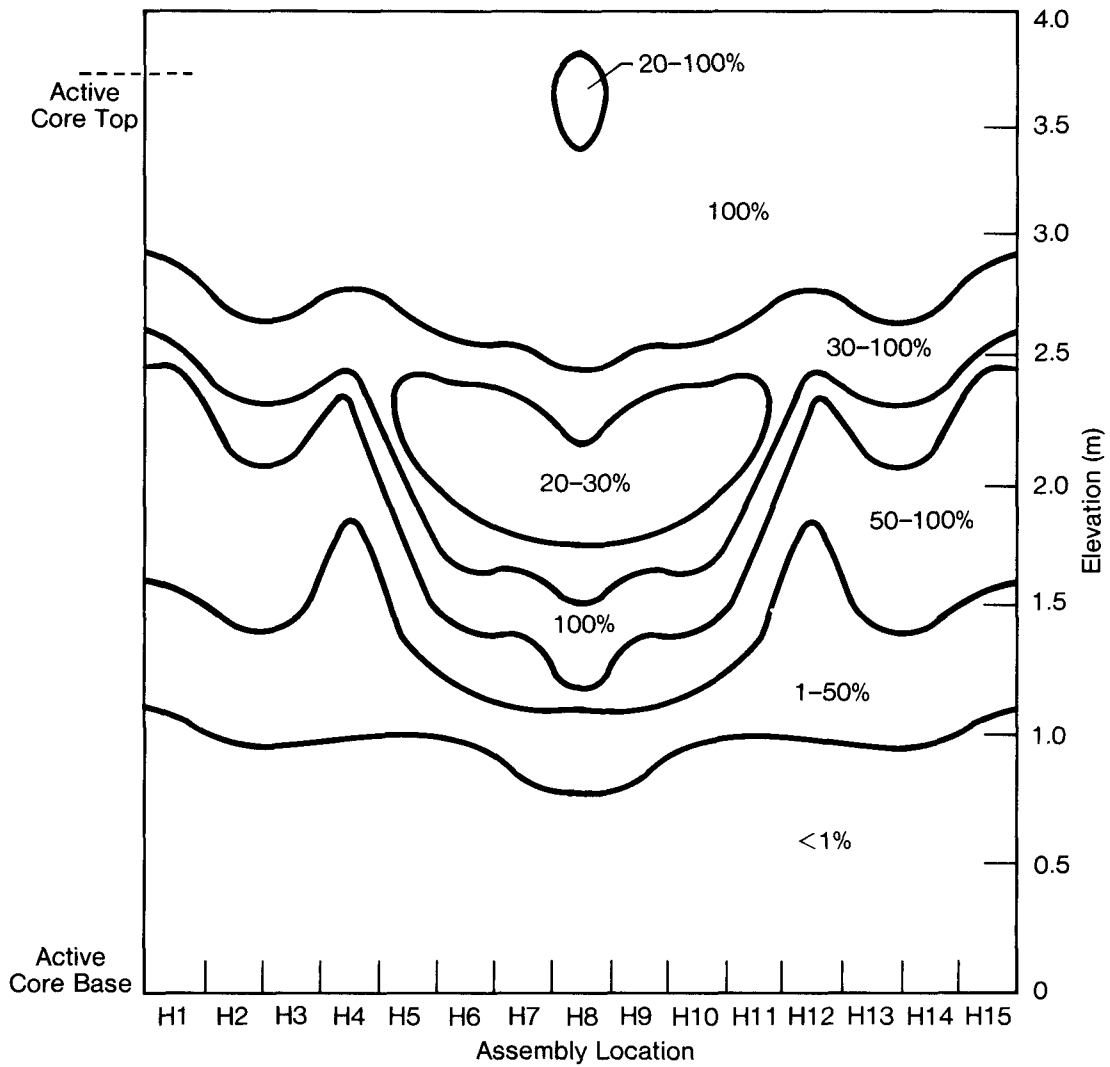


Figure 18. Calculated distribution of oxidized Zircaloy in core section H at $\tau = 208$ minutes. Percentages refer to fraction of clad oxidized.

that oxidation rates can be limited by steam starvation. Oxidation commences near the top of the core because this region is uncovered first. Subsequently, enhanced oxidation in the high power region in the lower half of the core consumes the oxygen in the rising steam, and tends to limit the rate of reaction in the core center.

Calculations indicate that over the entire period of uncovering, none of the fuel exceeded the UO_2 pellet melting temperature ($2790^{\circ}C$). Furthermore, less than 30% of the fuel in the core exceeded the clad melting temperature ($1850^{\circ}C$), which is the minimum temperature needed for the formation of significant amounts of liquid U-Zr-O alloys.*

4.2 Sensitivity to Input Assumptions

To estimate the sensitivity of the predicted core oxidation levels to the major modelling assumptions a series of parametric variations were carried out.

Calculations were made with the following assumptions:

- (i) convective heat transfer coefficients increased by a factor of five;
- (ii) level time history in Fig. 7 changed by ± 15 cm;
- (iii) level time history calculated on basis of maximum steam condensation ($n = 1$) and zero condensation ($n = 0$), on the incoming make-up flow (see Fig 7);
- (iv) adoption of the Baker-Just [47] correlation for oxidation rates; (as seen in Fig. 11 this equation tends to somewhat over-estimate measured oxidation rate data);
- (v) zirconium oxidation not limited when subchannel steam flow is calculated to be zero (no steam starvation limit);
- (vi) zirconium oxidation is terminated on inception of clad melting, as postulated in [3].

Results of these calculations, shown in Table 5, are expressed in terms of the core state at 202 mins., just prior to HPI initiation. The oxidation fractions given refer to zirconium within the fuelled region only (nodes 1-32).

*U-Zr-O alloy formation is dependent upon temperature ($>1350^{\circ}C$), intimate pellet and cladding contact, and oxygen content. At $2000^{\circ}C$ the ratio of pellet to cladding volumes contributing to alloy formation ranges from 0.25 to 2.0.[46] Given that 30% of the fuel reached the clad melt temperature at TMI and that (typically) 70% of the clad remained unoxidized by the time fuel had reached this temperature, the fractional core UO_2 participation in alloy melt is of the order of 0.02 to 0.12. The dissolved oxygen in unoxidized cladding material is likely to bring the actual figure closer to 0.02.

TABLE 5

CASE	% zirc. oxidation in active core	Peak clad temperature (°C)
Reference case	28.0	2670
Level height increased by 15cm in boildown	7.5	2330
Level height reduced by 15 cm in boildown	37.1	2780
Level height calculated with n=1	11.5	2270
Level height calculated with n=0	30.5	2680
Nusseltnumber increased by factor five in eq (15) and (16)	22.4	2415
Oxidation rate correlation of Baker-Just adopted in favor of (22)	30.7	2540
Zero steam-starvation	39.5	2790*
Oxidation terminates on clad melt- ing	24.3	2280

TABLE 5 - Sensitivity of calculated core damage at 202 mins. to varia-
tions in input assumptions.

(*UO₂ pellet melting temperature)

It is seen that the zirconium oxidation fraction is greatly reduced by a small increase in make-up flow. This is because of the unstable nature of the exothermic oxidation process, which can cause a runaway heating effect when clad temperatures exceed about 1500°C. For the cases in Table 5 in which widespread oxidation is calculated, the assumption of oxidation inhibition by steam starvation appears to have the greatest effect on calculated damage levels.*

4.3 Calculated Temperature Transient in the Upper Plenum Region

The model was used to estimate the mean temperature and flow rate of the gas, and the metal-work temperature, in the vessel upper plenum region, (thermal and geometric properties of the non-fuel regions are given in Table 1). Fig. 19 shows the calculated time variation of the mean gas temperature in the upper plenum, at the elevation of the hot leg nozzles (which are located 4.6 m above the base of the active core). The temperature is a cross-section area-mean value obtained by averaging over the eight radial zones. Also shown in Fig. 19 is the total calculated gas flow at the same elevation. It is seen that the calculated gas temperature does not exceed 1300°C and is only briefly greater than 900°C. As would be expected the temperature time variation is strongly affected by the magnitude of the core exit flow. These findings are generally consistent with heat transfer studies of the A loop hot leg piping and instrument response [45].

As shown in Figs. 16 and 17, the calculations indicate that during the period of uncovering, metal-work in the upper plenum region is heated only a few degrees centigrade by the hot gases emanating from the core. However it is clear that this is unlikely to be true for the steel in the assembly end-fittings and upper core tie-plate, which is exposed to direct thermal radiation from the fuel rods, and would probably be very much hotter. Since radiative heat transfer is not included in the present analysis, a detailed estimate of the temperature in this region has not been attempted.

4.4 Comparisons with Indicated Level of Core Damage

Indications of the level of core damage can be obtained indirectly from instrumentation behavior, measured levels of fuel fission product release, and hydrogen generation. Present indications are as follows.

*This is in reference to maximum damage; other assumptions such as $\eta=1$ for the entire period have greater consequence relative to minimum damage predictions.

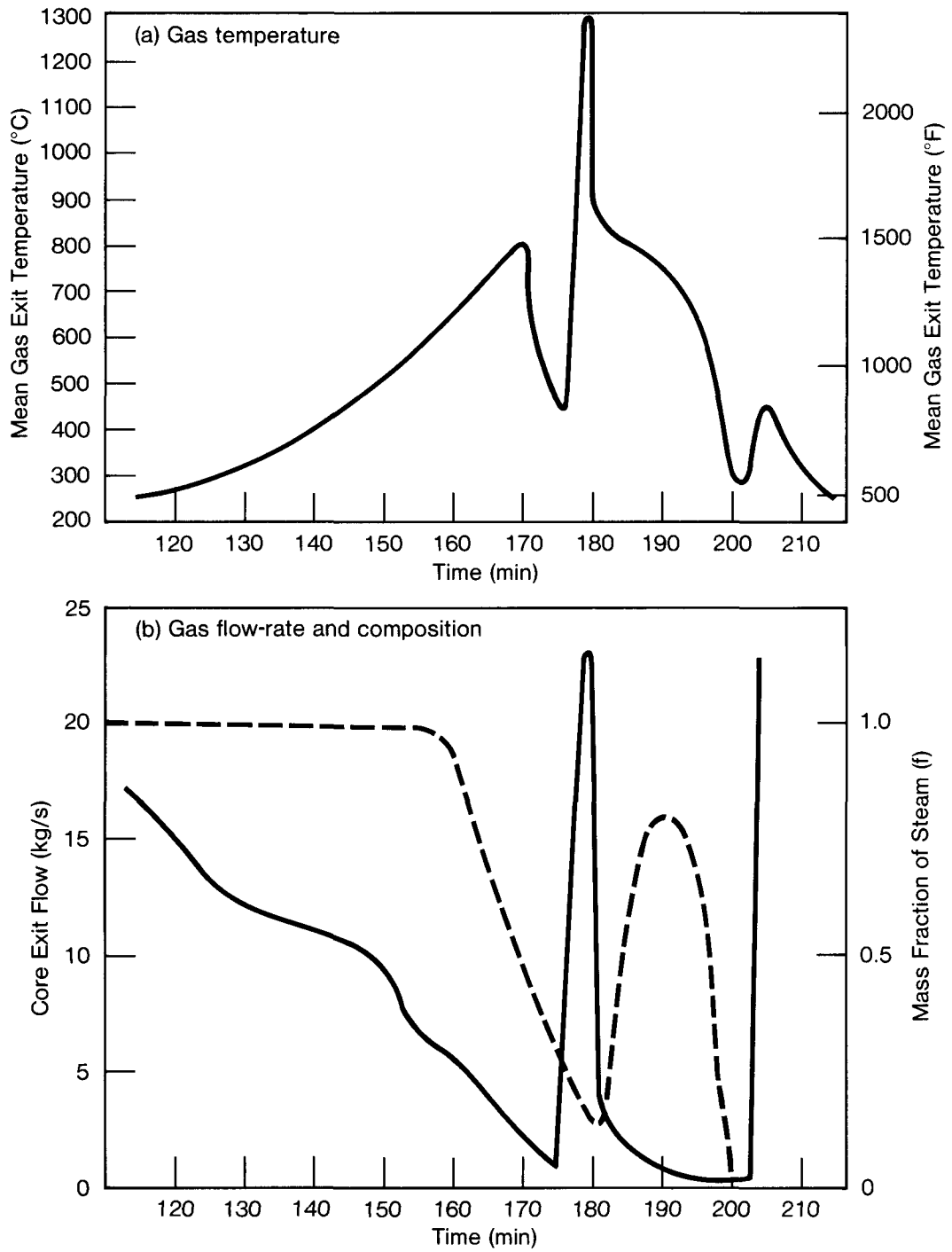


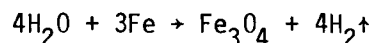
Figure 19. Calculated time variation of mean gas temperature, flow rate and steam fraction in the upper plenum at the elevation of the hot leg nozzles.

4.4.1 Hydrogen Generation

Considerable quantities of hydrogen were generated during the accident, and the containment pressure spike at $\tau = 590$ mins. was caused by partial deflagration of this hydrogen gas [1]. Probably the most reliable estimates of the quantity of hydrogen released are provided by the analyses of containment air samples taken in the months following the accident; measured levels of oxygen depletion in these samples can be used to estimate the quantity of hydrogen involved in the burn. The composition of the four air samples given in [1] imply that the mass of released hydrogen is in the range 300-550 kg, with a median estimate of 480 kg.

Possible sources of hydrogen that have been suggested are radiolysis [49], or the high temperature reaction between steam and the zircaloy or stainless steel. Theoretical calculations suggest that the quantity of radiolytic hydrogen generated in the TMI accident was negligibly small [50].

To determine the net hydrogen generation implied by the distribution of oxidized material shown in Fig. 18, use was made of the core material inventory data in Table 6 [43]. These data show that the approximate mass of Zircaloy-4 in and above the fuelled region is 22,670 kg. Since, 39% of the Zr-4 above the active core base is consumed in total, this implies a net hydrogen generation of 385 kg. In practice additional hydrogen would be expected to be formed by oxidation of some of the stainless steel within the fuel assemblies, which proceeds according to the equation [51]



at similar temperatures as the reaction between steam and zirconium. Assuming oxidation of 35% of the stainless steel in the active core length, and complete oxidation of the plenum springs in the fuel elements, generation of an estimated additional 50 kg of hydrogen is predicted. This brings the total estimated hydrogen production to ~435 kg, which is in reasonable agreement with the measurements given.

The slight underprediction of hydrogen generation could easily be explained by the assumption of a steam starvation oxidation limit. In practice recirculatory gas flows carrying steam to the oxygen starved regions may well have been possible in a large open core in the near stagnant conditions of the boil down (typical flow

TABLE 6

<u>CATEGORY</u>	<u>FORM</u>	<u>COMPOSITION</u>	<u>VOLUME</u> (ft ³)	<u>WEIGHT</u> (lb)
Fuel	ceramic pellets	UO ₂	324.3	205140
Absorbers	metal alloy rod ceramic pellets ceramic pellets	Ag-In-Cd B ₄ C in Al ₂ O ₃ Gd ₂ O ₃ -UO ₂	9.55 7.29 0.46	6060 380 290
Structures	fuel cladding guide tubes instrument tubes control cladding poison rod cladding orifice rod cladding spacer grids spacer sleeves plenum springs ceramic spacers metallic spacers end plugs end plugs	Zircaloy-4 Zircaloy-4 Zircaloy-4 304SS Zircaloy-4 304SS Inconel-718 Zircaloy-4 (stainless) ZrO ₂ (stainless) 304SS Zircaloy-4	109.7 6.65 0.62 2.70 4.04 0.13 5.24 0.64 3.10 2.13 0.90 0.28 3.69	44440 2690 250 1350 1640 60 2670 260 1550 730 450 140 1490
Trace	SPND T/C background detector neutron source instrument thimble clad instrument calibration tube insulation	rhodium-inconel chromel-alumel (cobalt) Am-Be-Cm inconel (inconel) (ceramic)	- - - - - - -	- - - - - -

TABLE 6 - Materials inventory in core, excluding assembly end fittings (source ref. 43)

velocities are of the order of ~5 cm/sec). Since ample steam was available in the vessel above the core it is possible that steam starvation may not have occurred to the extent indicated in the present analysis. Note that in the absence of steam starvation the calculated hydrogen production would increase by an additional ~90 kg. (cf. Table 5).

4.4.2 Fission Product Release

Fission product release levels may also be used to obtain an indication of the aggregate fuel damage. Since the occurrence of the TMI-2 accident, numerous gas and liquid samples have been taken from the RCS and from the containment atmosphere and sump. The most complete summary of the composition of these samples is reported in [52]. Table 7 contains a list of the range of estimated fission product release levels suggested by sample analyses reported in refs. [52,53,54,55].

To establish if the fission product release level in Table 7 are compatible with the core thermal transient calculated in Section 4.1, some appraisal must be made of the mechanisms by which fission products are released from overheated fuel. A brief description of release mechanisms is given below:

- (i) Gap release. After clad failure, gaseous and volatile fission products resident in the clad gap and rod plenums are released immediately. Typical gap release fractions [56] are listed in Table 8.
- (ii) Diffusion. During heating, subsequent to clad failure, further gaseous fission products are released by diffusing through the solid UO_2 matrix. Models describing this process are discussed in [57]. Table 9 provides appropriate time/temperature release data obtained experimentally by Lorenz [58].
- (iii) Pellet Melting/Liquifaction. Pellet melting leads to rapid release of fission products. Typical temperature time release data are given in Table 10. In the presence of Zr-4 fuel cladding, fuel liquifaction can occur at comparatively low temperatures by the formation of U-Zr-O alloys (see Sections 3.3 and 4.1). Lorenz [58] has suggested that release rates from alloy compounds are comparable to those for liquified fuel, but this does not yet seem to have been experimentally confirmed.
- (iv) Fuel Sintering. Growth of fuel grains at elevated temperature ($>1650^\circ C$) is a recognized mechanism for enhanced fission product release [60]. The oxygen potential is the basic parameter governing the sintering rate at a given temperature. Cubicciotti [61] has recently proposed a model for gaseous and volatile fission product release to account for grain growth effects, enhanced by steam. Using this model and the temperature history developed in the present analysis, a gaseous fission product release fraction on the order of 0.4 has been computed [62].

Table 7

Activity Releases for TMI(2) Fuel

<u>Nuclide</u>	<u>Core⁽¹⁾ Inventory, Ci</u>	<u>Activity Released from Fuel, Ci</u>	<u>Percent Release</u>
85Kr	9.7x10 ⁴	4.6x10 ⁴ -6.8x10 ⁴	47 ⁽²⁾ -70%
133Xe	1.5x10 ⁸	6.3x10 ⁷ -9.9x10 ⁷	42 ⁽²⁾ -66%
131I	7.0x10 ⁷	2.9x10 ⁷ -3.9x10 ⁷	41-55% ⁽³⁾
137Cs	8.4x10 ⁵	3.8x10 ⁵ -5.1x10 ⁵	45 ⁽⁴⁾ -60%
90Sr	7.5x10 ⁵	<6x10 ²	<.08%
140Ba ⁽⁴⁾	1.4x10 ⁸	1.8x10 ⁶ -3.5x10 ⁶	0.1-0.2%

- *NOTES:
- (1) Based on calculations using ORIGEN code. Ref. [71]
 - (2) Met. Ed. containment air sample 5/3/79. Ref. [54]
 - (3) Iodine release has been inferred from cesium release fraction Ref. [52]
 - (4) Containment sump sample 10/20/79; lower value probably more appropriate because of leach-out. Ref. [54]
 - (5) Based reported measurements reported and estimated 3.1x10⁵ gal. cont. water. Ref. [55]

- (v) Pellet Cracking in Cooldown. There is some evidence that pellet cracking during cooldown may substantially increase overall diffusion release levels, although this process is not yet quantitatively understood. Parker and Barton [60] describe tests in which sudden cooling of fuel pellets produced fission product releases exceeding those observed in the pellet heating phase. Powdering of UO_2 fuel pellets along the grain boundaries has been observed during fuel quenching in tests at PBF [64]. Croucher [65] has suggested that grain boundary fracturing would be possible when the fuel is cooled from temperatures exceeding a threshold value of $1620^\circ C$. Fuel fragmentation would enhance diffusion and increase the leaching of soluble fission products from the fuel after core refill.

Examination of the core temperature transient calculated in Section 4.1 (see Figs. 16 and 17) suggests that over the entire period of uncovering less than 30% of the fuel in the core exceeded the zircaloy melt temperature $1850^\circ C$ ($3360^\circ F$) and that no fuel exceeded the UO_2 pellet melting temperature $2790^\circ C$ ($5050^\circ F$).* Thus the implied potential for significant fission product release from liquified fuel is small. This is consistent with the levels of Ba and Sr observed in the coolant samples (see Table 7) which are much lower than would be expected in the presence of substantial and sustained fuel melting (see Table 10).

The gap releases listed in Table 8 and the release rates for diffusion processes shown in Table 9, are too small to explain the observed release levels for gaseous and volatile fission products, given our calculated heating transient. In particular, if the sole release mechanism is simple diffusion, the measured levels of ^{85}Kr , ^{131}I and ^{137}Cs would imply that upwards of 50% of the fuel mass was baked at temperatures exceeding $2000^\circ C$ for a period of more than one hour.

Further studies of fission product release mechanisms are plainly needed before conclusions on TMI-2 fission products can be stated with confidence. Presently it appears that the dominant release mechanism is grain growth (fuel sintering) in steam. This process would certainly have been augmented by pellet cracking which may have occurred as the fuel was quenched. Some additional release may be attributed to the gap release, fuel liquification and simple diffusion, although it would appear that these release mechanisms played a much less important role.

Our analysis can readily justify gaseous and volatile fission products release fractions on the order of 0.45 - 0.55. This range is somewhat on the low end of

*This conclusion is stated with less confidence in regard to the 10% of the core (Section 3.3) that was embrittled prior to the partial quench at 174 mins.

Table 8
Gap Release Component

<u>Nuclide</u>	<u>Approximate Activity Released From Fuel, Ci*</u>	<u>Percent Release (typical)</u>
85 _{Kr}	7.7×10^3	8%
133 _{Xe}	4.4×10^6	3%
131 _I	1.1×10^6	1.7%
106 _{Rb}	2.8×10^5	5%
137 _{Cs}	4.3×10^4	5%
90 _{Sr}	0.8	1.0×10^{-4}
140 _{Ba}	139	1.0×10^{-4}

* Release values are the product of core inventory derived from ORIGEN calculation [71] and best estimate gap release fractions obtained from [56].

Table 9
Fission Product Release by Diffusion
From UO₂ Matrix (Fragmented Cladding)* [58]

<u>Temperature (°C)</u>	<u>Xe, Kr</u>	<u>Cs, I</u>
1600°C	5%	10%
2000°C	37%	50%
2400°C	90%	95%

* Samples heated 5 hours; burnup: 1000 Mwd/MT.
These release values are somewhat higher than were reported by Parker and Barton [60].

Table 10
 Fission Product Release From
 Molten UO₂/Zr clad in an
 Oxygen Deficient Atmosphere*

Element	Xe, Kr	Cs, I	Ru	Sr	Ba
Release	46%	32%	0.15%	10%	9%

* Data derived from ORNL tests reported by B. W. Parker and R. A. Lorenz [63].
 Results were not corrected for the fraction of sample melted, which is
 approximately equal to the percent rare gas release.

estimates obtained from the plant data (Table 7). It is possible that hot spots which persisted in the core after refill contributed to the aggregate fission product release fraction. This is, however, a speculative consideration.

4.4.3 Instrumentation Behavior

Limited core exit thermocouple information is available for the time period covered by our analysis. Nevertheless, the trends in off-scale thermocouple alarms are consistent with the calculated core thermal transient (Section 4.1). When the alarm print-out was restored at 168 mins. it is apparent that all 52 thermocouples were off-scale high. The partial quench at 174 mins. is marked by a brief return of 10 - 15 thermocouples (located at the core periphery) back on-scale [14]. The subsequent boil-off and resumption of the core-wide heat-up was accompanied by off-scale trending of these thermocouples. Core refill, commencing at 202 mins., is indicated by a sharp drop in the number of off-scale thermocouples. The return of additional thermocouples back on-scale over an extended time period is indicative of a gradual cooling trend. [1,14]

Instrument survival provides some means for assessing core conditions. In the case of SPND's, only 37 of 364 SPNDs in the core were functional after the TMI-2 accident; 35 of the surviving instruments are located at the edges of the core, below the 1.3m level, [66]. Failure of many SPNDs may be linked to changes in core geometry as discussed in the following section.

Suprisingly, 49 of the 52 Chromel/Alumel core exit thermocouples (junctions located 15 cm above the core top) are now functioning normally [66]; this is despite the fact that the thermocouple leads pass downward through the active core via instrumentation tubes that also contain the SPNDs. (Instrumented fuel assemblies are located in each of the radial power zones as shown in Fig. 14, [1].)

Thermocouple survival provides convincing evidence that large scale melting and flow of fuel materials did not occur at TMI-2, which is consistent with the implications of our analysis. However, the heat-up calculations suggest that the thermocouple leads were exposed to temperatures well in excess of the 1350°C melting point of the Inconel forming the thermocouple sheath and the lead wires (see Figs. 16 & 17). Tests at ORNL have shown that thermocouples can survive temperatures exceeding the sheath melting point, although recovery to normal behavior is slow [67]. Instrument survival at these high temperature

conditions is not guaranteed, and further investigation of instrument survivability is required.

4.5 Core Behavior After 202 mins: End State Condition

As stated above, our calculations indicate that operation of the HPIS after 202 mins re-established cooling throughout the dry region and terminated the clad oxidation process. However, there is evidence of further core structural damage after this time. At 227 mins a violent thermal interaction appears to have taken place inside the core [1] causing a sudden 1.4 MPa (200 psi) increase in RCS pressure, back flow from the core to the loops, a sharp increase in ex-core neutron counts, and simultaneous failure of 30% of the in-core SPNDs [28].* The increase in system pressure implies that $\approx 2.4 \cdot 10^9$ J of energy was suddenly deposited in the coolant at this point [72].

The nature of 227 min event is not fully understood, but the most likely explanation appears to be a collapse of dry fuel from the top of the core (which was probably severely weakened by clad oxidation) into the lower liquid filled region. The hypothesis of a core structural collapse is consistent with an energy balance based on our estimates of the core condition prior to refill at 202 mins. Calculations give the water level at this time as $z_{\ell} = 0.5$ m (1.65 ft) and the core stored energy (defined as the energy released in bringing the fuel to T_{SAT}) as $3.2 \cdot 10^{10}$ J. An additional $3.0 \cdot 10^{10}$ J of energy was added in decay heating in the period 202-227 mins. Now HPIS was operated between 202-217 mins, after which make-up was negligible** until HPI was re-activated at 236 mins [1,10]. Based on known HPI pump characteristics the estimated core injection over the period 202-227 mins is calculated as $\approx 4.5 \cdot 10^4$ kg of which $\approx 2.2 \cdot 10^4$ kg is needed to fill the core from the 0.5m to the 3.6m elevation. The maximum energy removal by boil-off of residual injected coolant is

$$(4.5-2.2) \cdot 10^4 \cdot (h_{g\ell} + C_{\ell} \Delta T_{SUB,i}) = 5.6 \cdot 10^{10} \text{ J}$$

* During this period entire strings of SPNDs in the central core region went off-scale and never recovered. The rapid sequences of failures and the fact that SPNDs near the bottom of the core were affected for the first time in the accident suggest that these failures were mechanically induced. The actual mechanism(s) of failure have, however, not been positively established.

**Inferred from observations of make-up tank level and letdown flow.

This is less than (but close to) the sum of the stored energy and added decay heat (total $6.2 \cdot 10^{10} \text{J}$), implying that the core was only partly quenched by 227 mins. The calculated residual core stored energy, $6.0 \cdot 10^9 \text{J}$, is more than sufficient to account for RCS pressure rise in the 227 min event, which is consistent with the idea that a mass of dry material was suddenly quenched by collapsing below the liquid level. The implication is that a layer of ZrO_2 and UO_2 fuel pellet fragments was formed at this time, and now extends over most of the region above the core midplane.* Some displacement of fuel debris below the core and into other primary system low points may have also occurred.

Core behavior between 227 mins and re-establishment of forced circulation cooling at 949 mins is difficult to analyze because of the loss of core geometry, and absence of significant trends in core instrumentation response. However observations of the BWST level indicate that make-up in the period 227-545 mins was well in excess of the level required to replace coolant boiled-off by decay heat [10]. Also it is known that no significant clad oxidation/ H_2 production occurred after the hydrogen burn at 589 mins. This tends to suggest that a cooling trend was established after ~227 mins and core damage was essentially completed by this time. This is supported by the observation of a downward trend in the number of core exit thermocouples recording off-scale temperatures ($>390^\circ\text{C}$) after 202 mins. [1]

Temperatures above saturation continued to be registered by some core exit thermocouples even after forced circulation was re-established. There are several explanations for this behavior: (i) the core was maintained in an uncovered state; (ii) accumulations of fuel debris around instrument strings produced "virtual" thermocouple junctions at local hot spots, causing erroneous readings; (iii) instrument hysteresis after extended overheating. The prevalence of subcooled thermocouple readings at the core periphery after 300 mins [1], seems to rule out the first possibility (i.e., extended core uncovering). Virtual junction and hysteresis effects have been observed by Anderson [67] and seem to be the most likely explanation for the long term core exit temperature data.

*Compaction of core materials will be constrained by the packing fraction limit for fuel debris. Comparison between the theoretical packing fraction limit for equal spheres (0.68) and that of the as-built core (0.45) suggests an approximate upper-bound volume compaction of about 30%.

The thermocouple virtual junction effect and the very gradual cooldown implies significant thermal conduction lengths in aggregations of fuel debris. This observation qualitatively reinforces the view that substantial clad degradation and fuel dislocation did in fact occur[42].



Section 5

CONCLUSIONS

Best estimate calculations have been performed to determine the water level trajectory in the core, and the thermal transient experienced by the fuel and vessel internals, during the early period of core uncovering at the Three Mile Island (2) reactor. Results of calculations are consistent with core instrumentation response during the period of uncovering, and provide a reasonable explanation for the observed containment hydrogen levels and for the behavior of the ex-core thermocouples. However, the release levels of volatile and gaseous fission products are somewhat higher than would be expected from the calculated duration of the fuel temperature excursion.

5.1 Damage Sequence

The major events in the progression of core damage are as follows:

- (i) Core dry-out began at approximately 113 min. after reactor trip, the core heat-up transient continued through 202 min. The sustained high pressure injection beginning at 202 min. is thought to be the primary factor which halted the progression of damage.
- (ii) Evidence indicates that two make-up pumps were supplying coolant to the primary system during the early part of the boil-down (113-158 min.), but that the combined make-up flowrate was considerably less than the high pressure injection system design flow rate; substantial condensation/recirculation within the pressure vessel is believed to have occurred.
- (iii) Fuel pin cladding failures began to occur approximately 140 min. after trip.
- (iv) By 174 min. the core coolant level had dropped to about 1.0m from the active core base. Approximately 50% of the (active core) had been heated to temperatures at which rapid fuel cladding corrosion occurs.

- (v) The core heat-up transient was interrupted at 174 min. by the operation of the 2B reactor coolant pump, resulting in a partial quench; cladding embrittlement had not progressed to the point where wide spread shattering of fuel cladding occurred during this cooldown.
- (vi) Core temperatures began to rise after coolant injected into the core region (at 174 mins.) was boiled off.
- (vii) The core coolant level resumed its downward trend in response to near zero coolant make-up; a minimum level (estimated at 0.5m from the bottom of the active core) was reached at 202 mins. This is probably the lowest core coolant level over the entire accident period.
- (viii) The minimum coolant level at 202 min. coincided with the most severe thermal conditions experienced by the core; roughly 30% of the core had achieved temperatures in excess of the clad melt temperature (1850°C) by this time, with a peak temperature of 2650°C in the central fuel bundle.
- (ix) Manual initiation of high pressure injection (202 min.) terminated the core heat-up and clad oxidation process.
- (x) Embrittlement of fuel cladding and weakening of core support structures prior to reflood at 202 min. left the core in a vulnerable state; a significant mechanical disruption of the core appears to have taken place at 227 min., during cooldown.
- (xi) Fuel damage was stabilized by 230 minutes after reactor trip; the completion time for core refill and quench has not been definitively established.

5.2 Core End-State

Results suggest the overall core damage can be characterized as follows:

- (i) All fuel pins experienced clad failures (with the possible exception of pins on the core periphery that received sufficient cooling by radiative heat transfer).

- (ii) The core-wide zirconium oxidation was ~40%. More than 60% of the zircaloy materials in the core were significantly oxidized (> 1% local oxidation); the top-most regions of the core, particularly the fuel rod upper plenums, were fully oxidized.
- (iii) A significant fraction of the unoxidized fuel (~30%) exceeded the clad melting temperature during the transient; melting and refreezing of unoxidized cladding material on inner surfaces probably occurred.
- (iv) U-Zr-O alloy formation may have accompanied clad melt, but the extent of UO₂ participation is small in relationship to the total core UO₂ inventory (estimated at between 2 and 12%).
- (v) Fission product release analysis and the thermal-hydraulic analysis both indicate that negligible UO₂ pellet melting occurred.
- (vi) Steam temperatures in the upper plenum at the outlet nozzle elevation were generally below 900°C (1650°F), although this value was probably exceeded by the fuel quench caused by activation of the 2B reactor coolant pump, at 174 min. after trip; the metal work in the upper plenum, above the upper tie-plate, did not experience appreciable heating.
- (vii) A collapse and rubblization of fuel materials at the top of the core occurred at 227 min. after trip.

5.3 Areas of Uncertainty

Total clad oxidation was found to be very sensitive to the path followed by the water level in the core during uncovering; hence the main uncertainty in the analysis arises from uncertainties in the rate of water addition to the core by operation of the make-up system.

Examination of the effect of variations in modelling assumptions on calculated core damage levels suggested that other significant uncertainties are (i) the magnitude of steam condensation rates on the injected make-up flow (ii) ability of three dimensional core flows to provide steam to maintain rapid oxidation of overheated zircaloy (iii) localized core geometry changes.

Geometry changes during the heat-up period could have developed from: (i) control rod failure and dispersal of molten control material; (ii) clad break-up and fuel dislocation during quenching (especially the partial quench at 174 min.); (iii) penetration of molten zircaloy or alloy materials through the outer oxide layer of fuel pins. Prior to 202 mins. any significant geometry changes were likely to have been concentrated in the central core region, above the 3.0m level.

Acknowledgement

The authors wish to acknowledge the assistance provided by NSAC and contractor personnel in core damage assessment work. Particular reference is given to G. R. Thomas (NSAC), L. C. Oakes (Oak Ridge National Laboratory), D. Coleman (Nuclear Associates International), J. C. Robinson (Technology for Energy Corp.), A. R. Buhl (Technology for Energy Corp.), P. Bieniarz (Energy Incorporated), H. Warren (Babcock and Wilcox), J. Honekamp (Argonne National Laboratory), and P. Abramson (Argonne National Laboratory), R. Henry (Fauske Associates).

Appendix A

Calculation of Letdown Flows from Letdown Cooler Outlet Temperatures

The TMI-2 letdown coolers consist of two helical flow shell/tube heat exchangers. The thermal performance of these units is very similar to that of a simple counterflow heat exchanger [1,66]. During the period of the accident of interest both coolers were in service, and since the cooler outlet temperatures agree to within 2°C, both are assumed to have been performing identically.

In response to a step change in letdown (tube side) flow, the tube side outlet temperature approaches a new steady value asymptotically, with a time constant ≈ 4 minutes. The new tube side flowrate is calculated from the asymptotic temperature level by using a simple heat balance, as follows (c.f. [1]).

The heat transferred by each cooler is related to the inlet/ outlet temperatures by the equation:

$$q = \frac{\beta_c \{T_{t,i} - T_{s,o}\} - (T_{t,o} - T_{s,i})}{\ln \{(T_{t,i} - T_{s,o}) / (T_{t,o} - T_{s,i})\}} \quad (A1)$$

applicable to a counterflow heat exchanger, conductance β_c . An energy balance for the tube side and shell side flows gives:

$$q = W_t C_{\ell} (T_{t,i} - T_{t,o}) \quad (A2)$$

$$q = W_s C_{\ell} (T_{s,o} - T_{s,i}) \quad (A3)$$

Under normal operating conditions shell side flow and inlet temperatures are fixed at design levels

$$W_s = 25 \text{ kg/s} \quad (2 \cdot 10^6 \text{ lbs/hr}), \quad T_{s,i} = 35^\circ\text{C} \quad (95^\circ\text{F})$$

The design value of the conductance is $\beta_c = 6.5 \cdot 10^4 \text{ W/}^\circ\text{C}$ ($1.24 \cdot 10^5 \text{ Btu/hr.}^\circ\text{F}$). However, during the accident, multipoint records of the cooler outlet temperature, and measurements of letdown flow recorded on the plant hourly log, show that for $T_{t,i} = 288^\circ\text{C}$ (550°F) an outlet temperature of $T_{t,o} = 57^\circ\text{C}$ (135°F) corresponds to a flow $W_t = 4.0 \pm 0.3 \text{ kg/s}$ ($65 \pm 5 \text{ gpm}$). This implies that the conductance of the operating coolers had fallen to $\beta_c = 4.2 \cdot 10^4 \text{ w/}^\circ\text{C}$ ($0.8 \cdot 10^5 \text{ Btu/hr}^\circ\text{F}$), possibly as a result of fouling.

Using the above values for β_c , $T_{s,i}$ and W_s eqs. (A1) - (A3) can be solved iteratively to give W_t in terms of the asymptotic outlet temperatures $T_{t,o}$. (The inlet temperature $T_{t,i}$ is taken as the loop-A cold leg temperature). Results of these calculations are used to derive the letdown flow history shown in Figure 5.

Appendix B

Estimates of Steam Condensation Downstream of HPI Nozzles in the TMI-2 Cold Legs

In the period $\tau = 100-200$ mins. coolant makeup at TMI-2 is believed to have entered the RCS via the HPIS injection nozzle in the 1B loop. Fig. B1 shows the injection geometry.

If the mean heat transfer coefficient for steam condensation on the horizontal free stream is h_{COND} , the energy deposited per unit time in the stream, assuming saturated steam and a linear axial temperature profile in the liquid, is

$$\dot{\epsilon} = C_{\ell} W_i \Delta T_{SUB,i} \quad \zeta / (1 + \zeta / 2) \quad (B1)$$

where $\zeta = (h_{COND} p x / C_{\ell} W_i)$

The maximum rate of energy deposition is simply $C_{\ell} W_i \Delta T_{SUB,i}$: Thus the condensation efficiency is given by

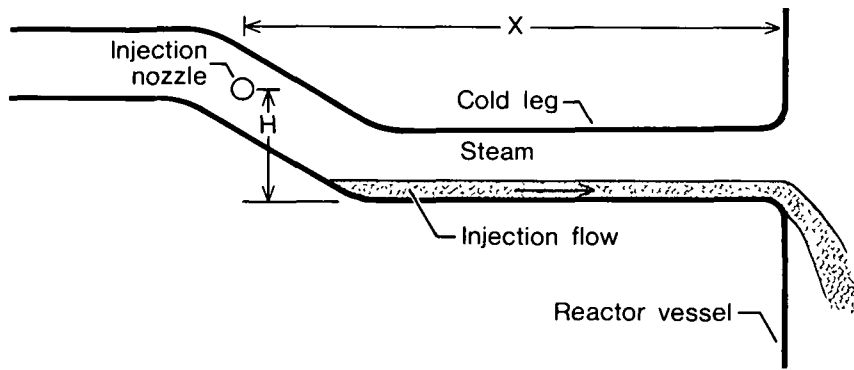
$$\begin{aligned} \eta &= \frac{\text{actual rate of steam condensation}}{\text{maximum rate of steam condensation}} \\ &= \zeta / (1 + \zeta / 2) \end{aligned} \quad (B2)$$

The condensation heat transfer coefficient is estimated using the mass transfer analogy suggested in refs. [69] and [70], which gives the relation

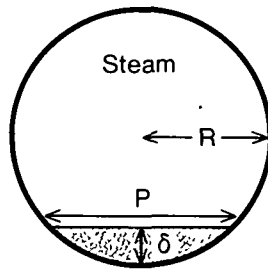
$$Nu_t = 0.25 Re_t^{0.75} Pr_t \quad (B3)$$

where Nu_t , Re_t , Pr_t are based on turbulence length and velocity scales.

$Nu_t = h_{COND} \lambda_t / k_{\ell}$; $Re_t = U_t / \nu_{\ell}$; $Pr = C_{\ell} \rho_{\ell} \nu_{\ell} / k_{\ell}$. From the open channel flow condensation experiments of [67] and [68] it has been found that, except for a short development length, condensation rates can be described using (B3) by setting



(a) Cold leg pipe work/injection path



(b) Section of cold leg pipe work

Figure B1. High pressure injection flow geometry at TMI-2.

$$\begin{aligned} U_t &\sim 0.3 U_\ell \\ \lambda_t &\sim \delta \end{aligned} \quad (B3^1)$$

from which, since $Pr^{1/2} \approx 1$

$$h_{\text{cond}} = 0.10 k_\ell U_\ell^{0.75} / (\delta^{0.25} \nu_\ell^{0.75}) \quad (B4)$$

For the present case Bernoulli's equation gives

$$U_\ell = \sqrt{2gH} \quad (B5)$$

It is calculated that $\delta \ll R$ in Fig. B1. Making use of this fact we have $\delta = P^2/8R$. Simple geometry then gives the following relationship between the stream depth and the flow-rate W_i

$$\delta^3 = W_i^2 / (2R \rho_\ell^2 U_\ell^2) \quad (B6)$$

Combining (B6) (B5) (B4) and (B1) we get

$$\zeta = 0.33 \frac{H^{7/24} x R^{5/12} g^{7/24} k_\ell}{\nu_\ell^{3/4} \rho_\ell^{1/6} C_\ell W_i^{5/6}} \quad (B7)$$

for the present case

$$\begin{aligned} H &= 0.89\text{m} & k_\ell &= 0.69\text{W/m}^2\text{K} \\ x &= 5.0\text{m} & \nu_\ell &= 2.2 \cdot 10^{-7}\text{m}^2/\text{s} \\ R &= 0.36\text{m} & \rho_\ell &= 900\text{kg m}^{-3} \\ & & C_\ell &= 4.5 \cdot 10^3 \text{J/kg}^0\text{K} \\ & & W_i &\approx 7 \text{kg/sec} \end{aligned}$$

Which gives

$$\eta = 1.0$$

Indicating that the condensation efficiency is just sufficient to bring the free stream to saturation temperature.

This calculation can be used as a rough indication that some steam condensation probably took place on the injected flow. However it must be emphasized that eq(B3) and (B3¹) is only supported by a limited data base, and the numerical calculations for η could easily be in error by a factor of two.

REFERENCES

- [1] EPRI Report NSAC-80-1, Analysis of the Accident at TMI-2, March 1979.
- [2] Presidents Commission report on accident at TMI-2, J. G. Kemeny et al, Oct. 1979.
- [3] NRC Inquiry Group, M. Rogovin Director, TMI Report to Commissioners and Public, Vol. II, Feb. 1980.
- [4] Meyer, R. O., Core Damage Assessment for TMI-2, NRC Memorandum to R. J. Mattson, NSAC File No. ANA-CO-0013, April 1979.
- [5] Ardron, K. H. and Cain, D. G., Modelling of the Liquid Level During Uncovery of the TMI-2 Core. Paper presented at the ANS/ENS Meeting on Thermal Reactor Safety, Knoxville, TN, April 1980.
- [6] Ardron, K.H. and Hall, P.C., Prediction of Void Fraction in Low Velocity Vertical Bubble Flows, Trans ASME J. Heat Transfer 102, p.(1 - 8) 1980.
- [7] Cunningham, and H. C. Yeh, Experiments and Void Correlation for PWR Small Break LOCA conditions, Trans. ANS, 1973.
- [8] Shumway, R. W, Loomis, G. G., Larson, T. K., Semiscale Simulations of the TMI transient INEL Report SEMI-TR-010, July 1979.
- [9] Larson, T. K., INEL, Private Communication, Dec. 1979.
- [10] Honekamp, J., Analysis of the Make-up Tank Level History Through 3:25, memo to Caldwell and Martin, 24 September 1979.
- [11] USNRC Report NUREG-0600, Investigation into March 28 Accident at TMI, Office of Inspections and Enforcement, Aug. 1979.
- [12] GPU Microfilm Record OPCP-2-803.
- [13] GPU Sequence of Events Report, Revision 2, Dec. 1979.
- [14] Output of TMI-2 Utility Printer. GPU Microfilm Record OPS-2-806.3274.
- [15] Transcript of NRC IE TMI Investigation Interview, W. Zewe, April 23, 1979, p.58-59. NSAC file/NRC-00-0096.
- [16] Transcript of NRC IE-TMI Investigation Interview, G. Kunder, April 25, 1979, p.57-59. NSAC file/NRC-00-0107.
- [17] Merchant, J., B&W. Telephone conversation with G. Martin, NSAC, Sept. 1979.

- [18] Lanese, L., GPU, Private Communications, Sept. 1979.
- [19] Cain, D. G., Examination of the Possibility of Letdown Flow Diversion on the Basis of MUT Level Perturbations at 174 Minutes. NSAC file memorandum ANA-CO-0050, May 1980.
- [20] B&W Calculation File 32-1162065, June, 1979.
- [21] Fernandez, R. T., Sursock, J. P., Kiang, R. L., "Reflex Boiling Heat Removal in a Scaled TMI-2 System Test Facility", ANS/ENS Meeting on Thermal Reactor Safety, Knoxville, TN April, 1980.
- [22] Bojduj, W., B&W, Memo to G. Thomas, NSAC, Aug 1979.
- [23] Oakes, L.C., Analysis of Containment Radiation Monitor Response during the period of uncovering of the TMI-2 core, NSAC file memorandum ANA-CO-0049.
- [24] Picklesimer, M. L. "Bounding Estimate of Damage to Zircaloy Fuel Rod Cladding in the TMI-2 Core", NRC File Memorandum, June 1979.
- [25] Coleman, D. R., "FRAP-T5 Analysis of Fuel Rod Conditions in the TMI-2 Core." NAI/EPRI Report NAI-80-45, May 1980.
- [26] Warren, H. D., "SPND Thermal Currents in a Furnace" B&W/NSAC Report, TSA Agreement 79-240-2, July 1979.
- [27] Baldwin, M. N. and Warren, H.D., "SPND Currents in a Furnace and Gamma Ray Field" B&W/NSAC Report, TSA Agreement 79-307, February 1980.
- [28] Robinson, J.C., TMI SPND Offscale Trending, TEC Report to NSAC. File No. ANA-CO-0033, August 1979.
- [29] Cain, D. G., Analysis of SPND response to TMI-2 Core Uncovery and Heat-up. NSAC File Memorandum ANA-CO-0045, May 1980.
- [30] Buhl, A.R., Robinson, J.C., Slagle, F.J., 1980, TEC Report 9010, Rev 1.
- [31] Wooton, R. O. and Denning, R. S., BOIL. A Computer program to calculate core heatup in a coolant boil-off accident. Battelle Columbus Report, March 1975.
- [32] Abramson, et. al. "Status of the 'TMI Heatup' Code", ANL/LWR/SAF 80-1, May 1980.
- [33] Shaffer, C., "TMI-2 Reference Calculations and Sensitivity Studies Performed Using Boil2", Energy, Inc., Report to NSAC, 29 May 1980. NSAC File #ANA-CO-0065.
- [34] Knudsen, J. G., Katz, D. L., Fluid Dynamics and Heat Transfer, McGraw-Hill, NY, 1958.
- [35] Chexal, B. and Thomas, G. R. T., Calculation of Steam Hydrogen Mixture Properties at High Pressures and Temperatures. NSAC file memorandum, May 1980.

- [36] Thomas, G. R. , "Steam Depletion -- A phenomenological Rate Limit to Zircaloy Oxidation in a Power Reactor Uncovery due to Boiloff of Coolant Inventory", memo to E. Zebroski (NSAC), August 31, 1979.
- [37] Urbanic, V. F. and Hendrich, T. R., High Temperture Oxidation of Zircaloy-2 and Zircaloy-4 in Steam, J.Nuc. Mat., 75 p 251, 1978.
- [38] "A Study of Zircaloy-4--Steam Oxidation Reaction Kinetics," EPRI NP-225, Worchester Polytechnic Institue, September 1976; "A Study of Zircaloy-4--Steam Oxidation Reaction Kinetics", EPRI NP-734, Worchester Polytechnic Institute, April 1978.
- [39] Urbanic, V. F., Oxidation of Zirconium Alloys in Steam at 1000°C to 1850°C, ASTM-STP 633, 1976.
- [40] Cathcart, J.V., et al., Zirconium Metal Water Oxidation Kinetics. Reaction Rate Studies at ORNL, NUREG-17, August 1977.
- [41] Hagen, S., Granhager, A., Malauschele, H., Schulker, H., and Wallerfells, K., Experimentelle Untersuchung der Abschmelzphase von UO₂-Zircaloy Brennelementer bei versagerder Notkuhlung. Projekt Nucleäre Sicherheit Halbjahresbericht, 1977, KfK-2600, KfK, Karlsruche, Germany p 416-428.
- [42] R. Henry, Private communication to D. Cain (NSAC), critique of draft report, September, 1980.
- [43] Coleman, D. R., "Nominal Design and Material Characteristics of the TMI-2 Reactor Core and Adjacent Regions," NAI Report to NSAC, 25 March 1980.
- [44] Letter by Hiatt, R. M., to Mallay, J. F., B&W proprietary information on reactor vessel upper internal geometry, 9 April 1980.
- [45] Brown D., Butzin, D., "Primary Pipe Steam Flow Rate and Temperature Analysis, 112 minutes to 174 minutes", interim report, NSAC TSA-79-239, April 1980.
- [46] Thomas, G.R.T., Private Communication to K. Ardron, March 1980.
- [47] Chung, H.M., memot to J. Honekamp, "A Discussion on Reactions and Damage in Fuel Rods of the Three Mile Island - 2 Reactor", Argonne National Laboratory, 22 Aug. 1979.
- [48] L. Baker and L. C. Just, "Studies of Metal Water Reactions at High Temperatures. III. Experimental and Theoretical Studies of the Zirconium-Water Reaction," ANL-6548, May 1962.
- [49] Karwat, H., Munchen, Tu, "Zu Prognosen Uber den Kemzustand des TMI-2-Reaktors", Atomwirtschaft, Marz 1980, p. 129.
- [50] Conine, J. C., Krommenhock, D. J., Logan, D. E., "KAPL Evaluation of Radiolysis Associated with the Three Mile Island Unit 2 Incident. Attachment to letter by H. G. Rickover to R. L. Ferguson (DOE), 24 May 1979.
- [51] J. T. Bittle, L. A. Sjudahl, J. F. White, "Oxidation of 304L Stainless Steel by Steam and by Air," Corrosion NACE, Vol. 25 #1, Jan 1969.

- [52] Bishop, W. N., Nitti, D. A., Jacob, N. P., Daniel, J. A., "Fission Product Release from the Fuel Following the TMI-2 Accident," ANS/ENS Meeting on Thermal Reactor Safety, Knoxville, TN, April 1980.
- [53] Letter by D. Nitti to D. Cain, Containment Gas Samples, 15 May 1980. NSAC file #RAD-00-1370.
- [54] TMI Unit 2 Technical Information and Examination Program Update, EG&G, Idaho, Inc., 15 April 1980; Nitti, D. Private Communication with D. Cain, 14 May 1980.
- [55] Rickover, H. G., "Three Mile Island Emergency Response-Information Requested by the President's Commission, Bettis Laboratory Memo to file dated 21 May 1979, reactor coolant and gas sample results; 24 May 1979.
- [56] WASH 1400, Reactor Safety Study, An Assessment of Accident Risks in U.S. Commercial Nuclear Power Plants, Vol. VIII, App. A., Oct. 1975.
- [57] Cottrell, W. B., et. al., "Fission Product Release from UO₂", USAEC Report, ORNL-2935, Oak Ridge National Laboratory, 1960.
- [58] Letter by R. A. Lorenz (ORNL) to W. V. Johnston (USNRC), 18 June 1979. NSAC file #RAD-00-0046.
- [59] Rest, J., Johnson, C., "Grass-SST Analysis of Integranular Fission Gas Release and Discussion of Related Physical Phenomena in Fuel Subjected to TMI-2 Type Trnsients", ANL/LWR/SAF 80-3, May 1980.
- [60] Parker, G. W., Barton, C. J., "Fission Product Release" The Technology of Nuclear Reactor Safety, Thompson and Beckerley (ed.), p. 576, 1973.
- [61] Cubicciotti, D., "A Model for Release of Fission Gases and Volatile Fission Products from Irradiated UO₂ in Steam Environment NT Letter in Nuclear Technology (to be published), NSAC file #ANA-CO-0062.
- [62] Cubicciotti, D., "Fission Gas Release Fraction During Core Uncovery", memo to D. Cain, October 1980, NSAC file #ANA-CO-0063.
- [63] Parker, G. W., Lorenz, R. A., "Melting of UO₂ by a Centered Tungsten Resistor," USAEC Report ORNL-3401, ORNL, 1963, p 11.
- [64] Cook, B. A., NUREG ICR-0757, Tree-1333, EG&G Idaho, Inc., June 1979.
- [65] Croucher, D. W., "Possible Fuel Powdering in TMI-2" EPRI memo. 11 July 1979. NSAC file #RAD-00-1371.
- [66] Ackerman, J., "TMI-2 Reactor Core Status Instrumentation Data Package, TMI Industry Advisory Group 11 April 1979 NSAC file #ANA-CO-0006.
- [67] Anderson, R. L., Banda, L. A. W., "Investigation of the Validity of Thermocouple Temperature Measurements at Three Mile Island," NSAC project report (draft), June 1980, NSAC file #ANA-CO-0064.
- [68] Northrup, S., Graham Manufacturing Co., Telephone conversation with K. Ardron, NSAC, Jan. 1980.

- [69] Bankoff, S. G., Some Condensation Studies Pertinent to LWR Safety. Paper presented at EPRI Workshop on Basic Two Phase Flow Modeling in LWR Safety and Performance, Tampa, FL, Feb 28-Mar 2, 1979.
- [70] Thomas, R. M., "Condensation of Steam on Water in Turbulent Motion", Int. J. Multiphase Flow, 5, p. 1, 1979.
- [71] Canada, R. G., "EPRI TMI ORIGEN Calculation," Report by Technology for Energy Corporation to NSAC. 2 May 1980.
- [72] Anderson, L., Memo to L. Oakes, "Fuel Dislocation at 0747," 17 August 1979, NSAC File # ANA-CO-0050.
- [73] Roberts, R., B&W, telephone conversation with D. Cain, NSAC, January 5, 1981.





